

J-P
mix

NASA CR-130134

NTIS \$6.50

SOLAR WIND PHOTOPLATE STUDY

Burton W. Scott and
H.G. Voorhies
Perkin-Elmer Corporation
Aerospace Division
2771 N. Garey Ave.,
Pomona, California 91767

November 1972
Final Report for Period June 1970 - July 1972
Final Submittal

Prepared for
GODDARD SPACE FLIGHT CENTER
Greenbelt, Maryland 20771

Reproduced by
NATIONAL TECHNICAL
INFORMATION SERVICE
U.S. Department of Commerce
Springfield, VA. 22151

(NASA-CR-130134) SOLAR WIND PHOTOPLATE
STUDY Final Report, Jun. 1970 - Jul.
1972 B.W. Scott, et al (Perkin-Elmer
Corp.) Nov. 1972 88 p CSCL 03B

N73-14810

Unclas
G3/29 51284

| | | | |
|---|--|--|---|
| 1. Report No. | 2. Government Accession No. | 3. Recipient's Catalog No. | |
| 4. Title and Subtitle Solar Wind Photoplate Study | | 5. Report Date July 1972 | 6. Performing Organization Code |
| | | 8. Performing Organization Report No. | |
| 7. Author(s) Burton W. Scott and H.G. Voorhies | | 10. Work Unit No. 30008 | 11. Contract or Grant No. NAS5-11313 |
| 9. Performing Organization Name and Address Perkin-Elmer Corporation Aerospace Division 2771 N. Garey Ave Pomona, California 91767 | | 13. Type of Report and Period Covered Final Report June 1970 to November 1972 | |
| | | | |
| 12. Sponsoring Agency Name and Address National Aeronautics and Space Administration Goddard Space Flight Center Greenbelt, Maryland 20771 | | | |
| 15. Supplementary Notes | | | |
| 16. Abstract An ion sensitive emulsion detection system has been considered for use in a cycloidal focusing mass spectrometer to measure the various atomic species which comprise the solar plasma. The masses and energies of ions found in the solar wind are outside the range covered by previous studies of ion sensitive plates. Therefore an investigation was undertaken using ions chosen to simulate the conditions of interest. The responses of Ilford Q2 and Kodak SC7 emulsions were measured with N^+ ions at 6 keV to 10 keV, He^{++} ions at 750 eV to 2500 eV, and H^+ ions at 550 eV to 1400 eV. These ions have the approximate range of velocities (about 300-500 km sec ⁻¹) encountered in the solar wind. The work was carried out on a specially prepared magnetic sector mass analyzer. Characteristic response curves were generated, each one utilizing approximately 50 data points at three or more current densities. In addition to the ion response, measurements of the response of these emulsions to a photon flux simulating the visible portion of the solar spectrum were made. The results obtained will be presented in detail and interpreted in relation to other data available for these emulsions. | | | |
| 17. Key Words (Selected by Author(s)) Ion Detection Mass Spectrometry Solar Wind Detectors | | 18. Distribution Statement | |
| 19. Security Classif. (of this report) Unclassified | 20. Security Classif. (of this page) Unclassified | 21. No. of Pages | 22. Price* 6.50 |

PRECEDING PAGE BLANK NOT FILMED

THIS PAGE INTENTIONALLY LEFT BLANK

TABLE OF CONTENTS

| | <u>Page</u> |
|--|-------------|
| INTRODUCTION | 1 |
| DESIGN | 1 |
| TEST PROGRAM | 3 |
| Tests of Light Tightness and Vacuum Integrity | 3 |
| Tuneup of Source | 4 |
| Exposure and Development of Plates and Films | 4 |
| Darkroom Procedure | 5 |
| Densitometer Reading | 5 |
| RESULTS | 6 |
| Sensitivity to Ion Exposure | 6 |
| Error Analysis of Ion Exposure Measurements | 8 |
| Measurement of Ion Current | 8 |
| Identity of Ions, Beamwidth, Dispersion, and Resolution | 9 |
| Exposure Time | 11 |
| Ion Energy | 11 |
| Developing Procedure | 11 |
| Density Measurement | 12 |
| Image Size | 12 |
| Summary of Errors - Discussion | 12 |
| SENSITIVITY TO LIGHT | 14 |
| DEVELOPERS, FOG, AND MINIMUM DETECTABLE ION SIGNALS | 14 |
| CONCLUSIONS | 20 |
| APPENDIX A - ILLUSTRATIONS | 22 |
| APPENDIX B - MEASUREMENT OF CHARACTERISTIC CURVES FOR KODAK SC7 FILM AND ILFORD Q2 FILM | 65 |
| REFERENCES | 83 |

LIST OF ILLUSTRATIONS

| <u>Figure</u> | <u>Page</u> |
|--|-------------|
| 1 Mass Analyzer | 22 |
| 2 Block Diagram of Source, Analyzer, Cassette and Power Supplies | 23 |
| 3 Overall View of Mass Analyzer and Support Equipment | 24 |
| 4 Schematic of Electrode Arrangement of the Ion Source, Mass Analyzer, and Cassette | 25 |
| 5 A Typical Densitometer Trace Over a Set of Patches The Exposure Time Varies by x2 From One Patch to the Next | 26 |

LIST OF ILLUSTRATIONS (Cont)

| <u>Figure</u> | | <u>Page</u> |
|---------------|---|-------------|
| 6 | A Detailed Trace of a Single Patch on the Densitometer, Illustrating Typical Resolution and Uniformity | 27 |
| 7 | A Typical Patch of Very Light Density | 28 |
| 8 | H ⁺ Ilford | 29 |
| 9 | He ⁺⁺ Ilford | 30 |
| 10 | N ⁺ Ilford | 31 |
| 11 | H ⁺ Kodak | 32 |
| 12 | He ⁺⁺ Kodak | 33 |
| 13 | N ⁺ Kodak | 34 |
| 14 | Sensitivity of Ilford Q2 and Kodak SC7 as Functions of Energy for Various Ions | 35 |
| 15 | Sensitivity of Ilford Q2 and Kodak SC7 as Functions of Mass | 36 |
| 16 | Detail of the Exit Slits, Cassette, and Film Plate Holder | 37 |
| 17 | Collector Current as N ₂ ⁺ Beam is Swept Past Exit Slits by Varying the Accelerating Voltage | 38 |
| 18 | Exposures of Ilford Q2 Plates to the He ⁺⁺ - H ₂ ⁺ Doublet. | 39 |
| 19 | Trace of the Ion Current Due to the He ⁺⁺ - H ₂ ⁺ Doublet as the Beams are Swept by 0.012 Inch Exit Slit by Varying Accelerating Voltage | 40 |
| 20 | Typical Oscilloscope Traces of the Pulsed Ion Beam | 41 |
| 21 | Patch Width Spreading at Increased Current Levels | 42 |
| 22 | Sensitivity of Ilford Q2 and Kodak SC7 to Simulated Visible Solar Radiation | 43 |
| 23 | Background Fog Level With Various Developers and Times | 44 |
| 24 | H ⁺ Ilford (500 eV) | 45 |
| 25 | H ⁺ Ilford (1000 eV) | 46 |
| 26 | H ⁺ Ilford (1300 eV) | 47 |
| 27 | He ⁺⁺ Ilford (750 eV) | 48 |
| 28 | He ⁺⁺ Ilford (1650 eV) | 49 |
| 29 | He ⁺⁺ Ilford (2500 eV) | 50 |
| 30 | N ⁺ Ilford (6 keV) | 51 |
| 31 | N ⁺ Ilford (8 keV) | 52 |
| 32 | N ⁺ Ilford (10 keV) | 53 |
| 33 | H ⁺ Kodak (550 eV) | 54 |
| 34 | H ⁺ Kodak (1000 eV) | 55 |
| 35 | H ⁺ Kodak (1300 eV) | 56 |
| 36 | He ⁺⁺ Kodak (750 eV) | 57 |
| 37 | He ⁺⁺ Kodak (1650 eV) | 58 |

LIST OF ILLUSTRATIONS (Concluded)

| <u>Figure</u> | | <u>Page</u> |
|---------------|--|-------------|
| 38 | He ⁺⁺ Kodak (2500 eV) | 59 |
| 39 | N ⁺ Kodak (6 keV) | 60 |
| 40 | N ⁺ Kodak (8 keV) | 61 |
| 41 | N ⁺ Kodak (10 keV) | 62 |
| 42 | Kodak SC-7 Test Film (4 Sheets) | 71 |
| 43 | Ilford Q2 Test Film (2 Sheets) | 75 |
| 44 | Source Calibration | 77 |
| 45 | Results Using Wratten 48 Filter | 78 |
| 46 | Shutter Speed Measurements | 79 |
| 47 | Kodak Calibration Table | 80 |
| 48 | Digital Test Results (2 Sheets) | 81 |

INTRODUCTION

In a previous study of a Solar Wind Mass Spectrometer, NASA Contract Number NAS5-11156, it was shown that the cycloid tube was an ideal solution to the problem because of its perfect focusing over the range of energies and angles encountered in the solar wind. A useful instrument could be constructed which would focus over a velocity range of 300 to 500 km s⁻¹, particles having the mass/charge range of the solar wind. One critical problem with such an instrument, however, lies in the sensitivity of the ion detectors. When the time to perform the experiment is limited, a photographic plate detector appears attractive because all ions are measured simultaneously. An examination of available data indicates that the sensitivity of available ion sensitive emulsions is critical to the success of the solar wind experiment. However, precise calibration data for the sensitivity of these emulsions to ions of the solar wind has not been available in the past. This is because the main interest in photographic ion detectors has been toward different goals, primarily in connection with spark source mass spectrographs¹.

In this application, the ions studied are normally medium to high mass and their energies range up to a few tens of keV. When attempting to relate these results to the solar wind it becomes evident that the ions of interest lie well outside the range of mass and energy that has been studied and for which calibration curves exist. The solar wind has a velocity ranging from 300 to 500 km s⁻¹. This results in an ion energy of approximately 1 keV per M/Q, where M is the mass in u (amu) and Q is the charge in electron charge units. The ions thus studied were H⁺, M/Q = 1, at ~ 1 keV, He⁺⁺, M/Q = 2 at ~ 2 keV, and N⁺, M/Q = 14 at ~ 10 keV. The N⁺ was tested at only 10 keV and below instead of at 14 keV in order to simplify the design.

DESIGN

The mechanical design of the mass analyzer used to select the ions used in the photoplate calibration centered around the large electromagnet shown in Figure 1 and the block diagram of Figure 2. The magnet is capable

¹Reference 1, p. 83. This reference will be found in the bibliography.

of generating 5 kg in a gap 9 x 11 cm in area x 3 cm thick. For this application pole pieces were designed and fabricated which gave a gap of 6 mm over a smaller area of 35 cm². These pole pieces were designed to make a 90° sector with average radius of 7.5 cm. The maximum field now possible with the magnet is well in excess of the 7 kg which is the highest required field for this study (required for 10 keV N⁺). With respect to the 90° magnetic sector, the film cassette and ion source are located at an object distance of 11.25 cm and an image distance of 5 cm giving a magnification of -0.66.

Some of the hardware details are not shown in the schematic, but are more evident in Figure 1. The ion source is inside the housing at the right. The housing is mounted on the end of a large ceramic tube wrapped with black tape for light tightness. The entire housing is enclosed in the plastic box to protect the operator from high voltage. The lines extending from the insulating box are the source voltage leads and the gas inlet tube. The gas inlet tube is made of insulating plastic and the ion source power supply is enclosed in plastic. The circuit board mounted inside the insulating box is utilized to switch the source for timed short exposures. The film is mounted in the cassette at the left. The cassette includes a shutter which also acts as a current monitor before and after each set of exposures. When the cassette is mounted to the rest of the analyzer, the shutter lead is brought out through a shielded feedthrough so that the current can be reliably monitored with an electrometer.

An overall view of the analyzer and associated equipment is shown in Figure 3. The main vacuum system is in the rack supporting the magnet with the cold trap and the exhaust tube on the back. The auxiliary vacuum system mounted in the small cabinet in front maintains the sample gas at the desired pressure in front of the inlet leak. The ion source voltage supply, which is also mounted in an insulating plastic box, is located on top of the inlet vacuum system. The Keithley 610C electrometer, used for current readings, can be seen in front of the magnet.

The ion source used is identical to that designed for NASA contract NAS9-9799, except for some minor modifications to adapt it to the present problem. The general configuration and layout of the source is shown in Figure 4. The source was operated with a range of electron energies from 50 to 200 eV in order to generate the desired ion species. The mechanical configuration of the ion source, which is constructed so that a large differential pressure is maintained between the source and the overall vacuum system is not shown in Figure 4. The conductance of the source, limited by the ion exit slit and the electron gun aperture, is approximately 50 cc s⁻¹. The leak between the gas supply and the source has a conductance of approximately 10⁻⁵ cc s⁻¹ so that normal operation, utilizing a flow of 5 x 10⁻³ torr cc s⁻¹, with a gas supply pressure of

approximately 500 torr resulted in an ion source pressure of approximately 10^{-4} torr. Obtaining sufficient ion production was not a problem, in fact, there was the opposite problem of adjusting the ion beam downward to the smallest measurable quantity. The vacuum system used consists of a six inch diameter diffusion pump with a liquid nitrogen cold trap. An ion gauge was attached to an arm of the main vacuum chamber to monitor the vacuum during pumpdown, with the shutter closed. The vacuum was not monitored while the shutter was open to avoid fogging the film with the gauge filament. The ultimate vacuum capability of the system was 2×10^{-7} torr. Satisfactory operation was obtained by pumping down to 2×10^{-6} before heating the ion source filament. Light baffles were installed to trap the light from the filament which might cause film fogging.

TEST PROGRAM

The test program was divided into the following phases:

- (1) Tests of vacuum integrity and light tightness
- (2) Tuneup of ion source and analyzer
- (3) Exposure and development of photoplates
- (4) Reading the plates with a microdensitometer.

Tests of Light Tightness and Vacuum Integrity

The vacuum system was checked out by standard methods, using a helium leak detector and baking as well as possible. The entire system could not be baked because of the bulkiness of the large magnet. When the vacuum system was operational, a sample film (Kodak plus-X) was inserted in the cassette to check for light tightness. Samples were tested with and without heating the source filament. The tests without the filament assured that the large ceramic insulator and all the headers were light tight. The insulator was translucent and required a wrapping of black plastic tape to avoid fogging the film. The tests to determine fogging by the filament were ambiguous. It was soon apparent that the filament was not fogging the film, but nevertheless some film became fogged even much later in the program when procedures were well established. It was finally decided that the fogging was probably due to brief glow discharges occurring when the shutter was opened, and accumulated outgassing products of the film were allowed to come in contact with some electrodes with voltages applied. By careful control of pumpdown procedures and by removing all voltages whenever gas bursts were possible, this source of fogging was eliminated.

Tuneup of Source

Three modes of operation were required for the three ions to be used in this study. First, the H^+ operation did not present a problem since it is the only possible ion with $M/Q = 1$. For this ion the source was operated with 90 eV electrons, the normal energy for which the source was originally designed. Total emission current regulation was used with the electron gun, with the anode current monitored separately. The electron gun was thus tuned by adjusting the voltages applied to the various electron focus electrodes. After initial ion beam tuning by monitoring the electrode in front of the magnetic sector, the magnet was energized, and final tuning was accomplished by monitoring the ion beam at the shutter.

The He^{++} ions were similarly tuned in, but this time the ionizing energy used was 190 eV. This higher energy (approximately four times threshold potential)² is required to get adequate production of these ions. While examining the character of this beam at the shutter, an interference problem became evident. H_2^+ has a mass only 1/125 different than He^{++} . The background H_2^+ beam from the source, apparently from H_2O contamination, was sufficient to make an image which was resolved from the He^{++} image. This image, shown in Figure 5, was far more evident on the developed film than it was on the electrometer monitor as the beam was swept past the image slit. This made the alignment for He^{++} exposures very tedious. Finally, the N^+ beam was tuned up with 45 eV electron energy. This ionizing voltage,² at the threshold for production of N_2^+ is still approximately twice the threshold for production of N^+ . The source was difficult to operate below 50 eV because the extraction field for the ions distorted the low energy electron beam in the ionization region. As mentioned previously, however, intensity of the ion beam was never a problem in these studies, and it was possible to obtain useful beam intensities from the source at these low electron energies.

Exposure and Development of Plates and Films

For each of the ion species the exposure and development procedures were as follows. First, with the film mounted in the cassette and the cassette mounted to the vacuum system and evacuated, the ion beam was tuned by monitoring it on the shutter. The desired current was adjusted by varying the electron current in the ion source and by varying the pressure of the inlet system. With the accelerating voltage fixed, the ion beam was tuned into the exit slit in the horizontal plane of the magnet gap by adjusting the magnetic field, and aligned in the vertical

²Reference 2, p. 83. This reference will be found in the bibliography.

direction by adjusting the voltage applied to the vertical steering electrodes. When the beam was thus adjusted to the desired value and centered on the exit slit as monitored on the shutter, it was turned off at the source, the electrometer disconnected and the shutter opened. A series of exposures were then made by alternately pulsing the source and moving the photoplate behind the exit slit. A series consisted of 10 to 12 exposures varying from ten milliseconds to one or two minutes, doubling each step. When one set of exposures was complete, the shutter was closed and the electrometer reconnected and the current recorded again. In every case, the current was stable during the exposures to better than +5%. A second set of exposures was made on the same plate at the same energy but with a different current level. The voltage was then changed and the beam tuned in again with the magnet and steering at the new voltage. Three voltages with two current levels at each voltage and twelve exposures at each current level made a total of 72 exposures per film or plate. The film, thus exposed, was sealed in the cassette and carried to the dark room.

Darkroom Procedure

In the darkroom, the procedure was as follows: first, all solutions were adjusted to 20°C. Deep tanks were used to minimize air contact. The dark room was illuminated using a safelight with a 15 watt bulb and a Wratten 6B filter aimed at the ceiling. The development schedule was:

- (1) Distilled water rinse - 1 minute
- (2) D19 developer - 3 minutes
- (3) Stop Bath SB-5 - 30 seconds
- (4) Kodak Fixing Bath F-5 - 3 minutes
- (5) Rinse in flowing water - 10 minutes
- (6) Final distilled water rinse - 1 minute.

Densitometer Reading

After developing and drying, the density was measured on a Jarrell Ash Model 203 microdensitometer. The densitometer output was recorded with an X-Y plotter. An example of the output is shown in Figure 5. The densitometer has an adjustable aperture through which the density of the films and plates are read. This aperture was adjusted to a length of 0.5 millimeters and a width of 2.5 microns. The actual resolution of

the density plot was less than 2.5 microns because the film and plates were not held exactly in the focal plane of the instrument. The Jarrell-Ash was designed to hold a larger size glass plate. An adapter to hold the plates and films positioned them slightly high in the instrument and compensating focus was not possible. Figure 6 shows a slow scan over a single patch. The patch width was approximately 0.25 millimeters and the resolution of the scan was sufficient to accurately measure the density. The height of the sample patches was approximately two millimeters so three passes could be made over each patch and the average of top, middle and bottom taken in order to account for any nonuniformity. In most cases the patches were uniform to better than five percent from top to bottom. The output plots from the densitometer were read directly in percent blackening. To correlate the percent blackening with exposure, the patch dimensions were measured with a toolmakers measuring microscope. Typical numbers are:

- (1) Patch Size - 0.009 x 0.080 in
- (2) Ion Current - 4×10^{-14} A
- (3) Current Density - 8.61 pA cm^{-2}
- (4) Exposure Time - 0.98 s
- (5) Exposure Density - 8.44 pC cm^{-2}

At each voltage and current density the exposure time was varied by up to three orders of magnitude in steps of x2. At least two different current densities were used for each specie at each voltage.

A patch is shown in Figure 7. This patch was chosen from some of the less dense exposures so that the individual grains can be seen in both the image and the surrounding background fog.

RESULTS

Sensitivity to Ion Exposure

The resultant curves of percent blackening vs exposure in pC cm^{-2} are shown in Figures 8 through 13. For each curve an error bar is given showing the observed scatter in the data. Individual curves, including data points are included in Appendix A. The exposure in coulombs cm^{-2} , which gave 50 percent blackening for each curve is shown in Table 1. Note that in many cases the observed scatter in data is greater than the difference between adjacent curves. Possible causes for this are discussed in the next section. Sensitivity is often defined as the

TABLE 1.- Exposure, Picocoulombs per cm²
for 50% Blackening

| | | Ilford Q2 | Kodak SC7 |
|-----------------|----------|-----------|-----------|
| H ⁺ | 500 eV | 47 | 12.5 |
| | 1000 eV | 13 | 2.8 |
| | 1300 eV | 6.2 | 0.2 |
| H ⁺⁺ | 750 eV | 30 | 8.2 |
| | 1300 eV | 19 | 4.25 |
| | 2500 eV | 13 | 0.65 |
| N ⁺ | 6000 eV | 11.5 | 1.65 |
| | 8000 eV | 7.2 | 1.10 |
| | 10000 eV | 6.3 | 0.85 |

inverse of the exposure for 50 percent blackening expressed in ions cm^{-2} . It is reported that sensitivity per ion is independent of the charge state³ so that ions cm^{-2} is a more appropriate unit than coulomb cm^{-2} . In the case of the three ions studied here there is only one charge state for each species so there was no opportunity to study this parameter. The sensitivity, expressed in $\text{cm}^2 \text{ coulomb}^{-1}$ and $\text{cm}^2 \text{ ion}^{-1}$ is shown in Figure 14. The He^{++} data is multiplied by a factor x2 on the coulomb scale so that there is a constant factor between the two scales. To illustrate the mass dependence of the sensitivity, Figure 15 is used. Again, two scales are given, expressing the result in $\text{cm}^2 \text{ coulomb}^{-1}$ and cm^2 per ion, with the $\text{He}^{++} \text{ cm}^2 \text{ coulomb}^{-1}$ data multiplied by x2.

Error Analysis of Ion Exposure Measurements

A number of measurements contribute to the final calibration curves presented here. In this section, we will discuss each measurement, its precision and verifying tests that are made on each one.

Measurement of Ion Current.- Before and after each set of measurements, the ion current was monitored on the shutter collector which is approximately two millimeters in front of the plane of the film or plates. The current was measured with a Keithley Model 610C electrometer which had been calibration certified immediately prior to the program. The accuracy of measurements with this instrument is plus or minus one percent, exclusive of noise and drift. Most of the measurements were made with the electrometer in the Fast (feedback) mode of operation with the sensitivity at 0.01×10^{-11} A full scale. Measured currents were normally 0.4 to 0.8 full scale. The feedthrough used to measure the ion current was the same as the mechanical feedthrough for operating the shutter. The resistance to ground of this assembly measured greater than 10^{15} ohms, so errors due to leakage are less than 0.01 percent. The limiting factor in measuring the current was noise and drift. The noise limit to the precision with which the electrometer could be read was plus or minus five percent for the higher currents of approximately 10^{-13} A and plus or minus ten percent for the lower range currents of approximately 5×10^{-14} . The drift of the source/electrometer combination during each set of measurements was not discernable through the noise. The zero level of current was measured by switching the ion beam off at the source. A retarding voltage of 100 volts was switched on to the ion exit aperture, thus providing a true zero reference regardless of zero offsets or leakage currents of any origin. Throughout the program Perkin-Elmer strived to utilize extremely small currents because of the extreme sensitivity of the films and plates. One such film was exposed with a current of 4×10^{-15} A and noise of $\pm 2 \times 10^{-15}$ A.

³Reference 3, p. 83. This reference will be found in the bibliography.

The exit slits, shutter and film are shown in Figure 16. A series of measurements were made to determine how to suppress secondaries in order to make accurate measurement of the ion current at the shutter. In addition to secondaries at the collector it was found that under certain conditions ions striking an electrode immediately adjacent to the slit could generate secondary electrons which could then loop through the exit slit causing a negative current at the collector. The most serious problems occur with He^{++} because of its high ionization potential. The secondary electrons produced by these ions have up to approximately 45 volts of energy. The potentials shown in the figure succeeded in suppressing both kinds of secondaries. A plot of collector current versus ion accelerating voltage as a beam of N_2^+ was swept past is shown in Figure 17. Also shown is a scan made without the negative suppression voltage. Apparently, the secondary coefficient is approximately twenty percent. The trace that results when the secondary suppression voltage on the middle electrode is used with the top electrode grounded is not shown in Figure 17. In that case, a small negative peak is found on each side of the positive ion peak. With 100 volts on the top electrode, secondary electrons generated there cannot pass to the collector.

Identity of Ions, Beamwidth, Dispersion, and Resolution

The H^+ ions were produced by using pure hydrogen in the inlet system and hydrogen diluted with helium. The energy of the ionizing electrons was adjusted to 90 eV. Since there is no possibility of other ions at $M/Q = 1$, the identity of H^+ is assured.

The He^{++} ions were produced with pure helium in the inlet system and with 190 eV ionizing electrons. The threshold of ionization for He^{++} is 54 eV² and ionization reaches maximum efficiency in the vicinity of four times threshold. The H_2^+ peak was present due probably to background H_2O in the source. It was identified and resolved from the He^{++} by narrowing the slit. The problem was studied carefully, and slit width was adjusted downward to assure that H_2^+ did not contribute to the final measurements. The $\text{H}_2^+ - \text{He}^{++}$ doublet is discussed in greater detail below in the paragraph on resolution.

The N^+ beam was produced with pure nitrogen in the inlet system and with 45 eV ionizing electrons. The threshold for production of N^+ from N_2 is 24.3 eV. The threshold for production of N_2^+ is 43.5 eV. Because of difficulties in operating the electron beam at below 45 eV the source was occasionally operated at one or two volts above the threshold for N_2^+ . Since maximum ionization probability occurs at four times threshold, this

²Reference 2, see page 4.

implies an operating point at one percent of maximum production for N_2^{++} and 25 percent of production for N^+ . In addition, the maximum cross section for N^+ is approximately twice that for N_2^{++} . Thus, the maximum contamination of the N^+ beam by N_2^{++} is $1/25 \times 1/2 = 2\%$. These ions, having higher mass and equal energy could cause an error toward slightly decreased sensitivity.

The critical dimensions of the magnetic sector mass analyzer are:

- (1) Sector Angle, $\theta = 90^\circ$
- (2) Object Distance, $l_o = 11.25$ cm
- (3) Image Distance, $l_i = 5$ cm
- (4) Source Aperture, $S = 0.012 \times 0.020$ in
- (5) Source Divergence, $\alpha = \pm 2^\circ$
- (6) Trajectory Radius, $r_o = 7.5$ cm

From these data the magnification and mass dispersion were calculated as follows:

$$\text{Magnification, } M = \frac{-\cos \tan^{-1} \frac{l_o}{r_o}}{\cos \tan^{-1} \frac{l_i}{r_o}} = -0.666$$

Dispersion, D

$$D = \frac{1}{2} (r_o + l_i) \frac{\Delta V}{\Delta} = 6.25 \frac{\Delta V}{V} \text{ cm or, } 6.25 \frac{\Delta M}{M} \text{ cm.}$$

Some tests which illustrate the beam shape and dispersion were performed with the masses appearing at $M/Q = 2$. It was found that background H_2O in the system gave a line due to H_2^+ which is separated from He^{++} line by:

$$\frac{\Delta M}{M} = \frac{14.5}{2016} = 0.0072.$$

⁴Reference 4, p. 83. This reference will be found in the bibliography.

The dispersion calculated from the sector dimensions would indicate a separation of 0.0184 inch for these two lines. The measured separation on the plates is 0.021 inch (see Figure 18). A trace of the beam current as the doublet is swept past the exit slit is shown in Figure 19. An image of the ion exit slit, with the calculated magnification should measure 0.008 inch. Measured image widths throughout the program varied upward from this dimension, probably indicating the influence of aberrations and surface charging of the plates or films.

Exposure Time.- The exposure time was regulated by an electronic timing circuit which controlled the retarding potential applied to the ion exit apertures. Times could be adjusted to 2, 5, 10, 20, 50, 100, 200, 500, and 1000 milliseconds. Each step was calibrated first by observing the actual ion current at the collector with an oscilloscope as it was switched. The preamplifier of the oscilloscope did not have sufficient sensitivity for this measurement so the Keithley 610C was used as an amplifier. Response was thus limited to about two milliseconds with the Keithley on the 0.001×10^{-9} scale (using N_2^+ ions). The two and five millisecond steps were calibrated by the applied voltage measurements and the rest were calibrated with the direct beam measurements. Figure 20 shows the oscilloscope trace of the pulsed beam at 5, 20 and 50 milliseconds.

Exposure error due to errors in the exposure time were thus less than five percent.

Ion Energy.- The ion energy was measured accurately to the nearest volt by the sum of the 0.1 percent calibrated high voltage supply and the additional 150 volts in the ion source. There may be a small error because of the 10 volt difference in potential between repeller and accelerator. It is impossible to know exactly at what potential between these two the ions are born. The ± 5 eV uncertainty is at most less than one percent of the ion energy.

Developing Procedure.- The developing solutions were adjusted to $20^\circ\text{C} \pm 1/4^\circ\text{C}$. The time of development was controlled to within one second. Temperature of development is directly correlated with time. For the SC7 film and Kodak D19 developer $1/4^\circ\text{C}$ is equivalent to five seconds variation in development time³. This means that the developing action was controlled to within two percent.

³Reference 3, see Page 8.

Density Measurement.- The density was measured on a Jarrell Ash Model 21 microdensitometer. This instrument focuses a small light on the emulsion. The portion of the light passing through the image is picked up by a photodetecting device and amplified. Span and zero adjustments on the amplifier are available so that the output is adjusted to read full scale for an opaque image and zero on background fog. It thus reads out directly in percent blackening. The principal source of error in the technique of using this instrument lies in the noise and drift of the background fog. By recording the scan of each set of images, as was done here, these errors are minimized. By inspection of Figure 6, this error can be estimated at less than three percent.

Image Size.- The size of each image is determined by measurements with a toolmaker's microscope capable of precise measurements to 10^{-4} inch, approximately one percent of the image width of ten mils. A much larger error is actually present in this measurement because of the lack of sharp edges. This can be seen in Figure 7 as approximately ten percent of total image width. The edge of the image, for purposes of calculating image area, was taken as the point where the image blackness was one-half the maximum for that image.

Summary of Errors - Discussion.- Two types of errors were almost completely negligible for measurements of this type, being less than one percent. They were determination of ion energy and uniformity of development. Slightly larger errors of one to five percent are possibly present in determining the exposure time and blackness of each image. The largest errors, plus or minus five to plus or minus ten percent are possibly present in measuring the ion current and in determining the image size. In one extreme case of using extremely low currents, the error in determining current level was plus or minus fifty percent, which can be seen by inspecting the error bars in Figures 8 through 13. The observed scatter in data is greater than should be expected from the sum of these errors. Possible reasons for this can be found in an analysis of the physical structure of the films and plates and of their electrically insulating nature.

These two emulsions are prepared primarily for sensitivity to the far ultraviolet. Ultraviolet radiation, like ions, is strongly absorbed by the gelatin, which holds the silver-halide grains in a normal emulsion. In the Q2 or SC7 emulsion, the average grain size is a fraction of a micron. In the Q2 plates, the emulsion is extremely thin (about 2 to 4 microns). A large portion of the grains protrude from the emulsion and have only an extremely thin skin of gelatin facing the ions. This skin may be only 250\AA^5 . Of course, in both the background fog and

⁵Reference 5, p.83. This reference will be found in the bibliography.

in the image, the actual darkening is due to agglomerates. The Kodak-Pathe/SC5 film is manufactured by a centrifuging process. While it is still a liquid, the emulsion is coated on a temporary substrate and centrifuged, which forces the silver-halide grains to the bottom in a densely packed layer. When it has solidified, the emulsion is stripped and transferred to its permanent base with the silver-halide now outermost with almost no gelatin.

Because of the exposed nature of the silver-halide, the emulsions are extremely sensitive to physical abrasion. This caused special problems in loading the cassette and in the developing technique. The shipping containers, as well as the cassette, were designed so that the film could be handled without touching the surface of the emulsion. Ions of the energy used in this study have a range of only a micron⁶ or less in the emulsion so there is little probability that an ion would strike a silver-halide particle that is buried very deeply in the gelatin.

Two possible reasons are advanced for the fact that the data scatter exceeds the estimated error for these measurements. The first is the problem of the sensitivity being so extremely dependent on the length of the particle path through gelatin. Even slight variations in the preparation of the emulsion can greatly effect the sensitivity of the film. McCrea,⁷ using Fe⁺ ions of undefined energy has reported a variation of x6 on the exposure required to achieve 50 percent blackening between different production runs of the Q2 emulsions.

The second difficulty that has been reported and which may be operative here is the problem of charging up the emulsion. Woolsten⁸ had particular problems with low energy ions (< 2 keV) in the energy range of many of the exposures. Woolsten also reports that Kodak SC5 is worse in this respect than the Ilford plates. One technique considered for overcoming these problems is applying a conductive coating to the glass before the emulsion is transferred to it. Ilford reports that they have studied this technique, but it was abandoned because it degrades the emulsion in other ways.⁹

The amount of charging may be related to the patch size of the exposed emulsion, since a retarding potential immediately in front of the film would have a defocusing effect. The image width as function of total charge exposure and current density is shown in Figure 21. The patch broadening is shown as a function of the arrival rate as well as total exposure. With very intense beams, more than an order of magnitude more dense than those in Figure 21, secondary ions begin to appear. These ions do not present a problem with the current densities used in the

^{6,7,8,9}References 6, 7, 8, and 9, p. 83. These references will be found in the bibliography.

calibration exposures, but they can and do present a severe problem when using photoplates in practical problems where a very strong line is very close to a much weaker one. Cavard¹⁰ has shown that the grains exposed by these secondary ions are different from the grains exposed by primary ions. The image due to them can be suppressed by using special developers with a small loss in overall sensitivity.

In addition to charging of the film, and the normal nonconstancy of the emulsion sensitivity, it has been suggested that additional variability in sensitivity can be assigned to factors such as storage time before exposure, fading of the latent image after exposure and before developing, and various conditions during pumpdown, such as the amount of absorbed moisture, etc.¹¹

SENSITIVITY TO LIGHT

Since a mass spectrometer measuring the solar wind will be subjected to the intense visible radiation of the sun, there must be adequate light traps built in to avoid fogging the film or plates. In order to determine exactly how good these light traps must be, the sensitivity to light of the two emulsions was measured. The source was designed to simulate the visible portion of the solar spectrum. A complete description and results of these tests are included as Appendix B. A summary of the results is presented in Figure 22. The sensitivity of Kodak Tri-X, from Kodak reference sheets is included for comparison. The units of meters candle second, normally used in photometry are included in Figure 22.

DEVELOPERS, FOG, AND MINIMUM DETECTABLE ION SIGNALS

A study of the effect of various developers and times was included in the light sensitivity study. Detailed results are included in Appendix B. A few conclusions as they relate to minimum detectable ion signal are presented here.

The developers studied were Kodak D-19, D-8 and Microdol-X. The D-19 is the most widely used formulation and is recommended by Kodak for most scientific films and plates. Because of its universal use, it was chosen for use with the ion exposures, in hopes that these calibration curves would then be more generally useful to others. It was originally planned to study ID-13, a caustic hydroquinone developer

^{10,11}References 10 and 11, p. 83. These references will be found in the bibliography.

manufactured by Ilford and formerly recommended for use with the Q2 plates. Ilford, however, has stopped manufacturing ID-13 and now recommends D-19. Kodak D-8 is very similar in composition to ID-13 and so was included in this study. The third developer, included here for completeness, was Kodak Microdol-X, a slow acting fine grain developer. The composition of the developers is given in Table 2.

The effect of various developers and developing times on fog level is summarized in Figure 23 and Table 3. When comparing this figure with the calibration curves for ion exposure, remember that percent blackening has slightly different meanings on the two figures. On the calibration curves, background fog is designated zero blackening and opaque is designated 100 percent blackening. As shown in Figure 23, zero blackening is complete transparency, i.e., the densitometer reading when the plate is removed. Again, 100 percent black is opaque. The background fog is due partly to the glass or film backing as well as the fogged emulsion. To translate a blackening figure, S_1 , from one of the ion sensitivity scales to a figure S_2 , in Figure 23, the following relation can be used:

$$S_2 = S_1 (1 - B.G) + B.G$$

where B.G. is the background fog level.

The smallest reliable signal measured for each ion species is shown in Table 4. In some cases the minimum detectable may be less than the value shown in Table 4, but was not actually demonstrated in this program because of difficulties with the surface charging and low current monitoring.

The conclusion drawn from these results is that for most purposes the three minute development period for Kodak D-19 should be maintained. For increased dynamic range, D-8 or Microdol-X can be used with some loss in sensitivity.

Other darkroom practices unrelated to the sensitive characteristics of the film may also affect the fog level. Included in this category are such things as a distilled water bath immediately prior to development. This bath removes some soluble silver ions from the emulsion which may cause fog¹². Another precaution is minimizing the exposure to air (oxygen) during the developing processes¹³. This is accomplished by using deep tanks instead of shallow trays and by going from one solution to the next rapidly.

^{12,13}References 12 and 13, P. 83. These references will be found in the bibliography.

TABLE 2.- Developer Formulations

| KODAK DEVELOPER D-8 | | | | |
|---------------------------------------|---------------------------|--------|----------------------|------------|
| | Avoirdupois-U.S. Liquid | | | Metric |
| | Water, about 90°F (32°C) | 24 | ounces | 96 ounces |
| Kodak Sodium Sulfite, desiccated | 3 | ounces | 12 ounces | 90.0 grams |
| Kodak Hydroquinone | 1-1/2 | ounces | 6 ounces | 45.0 grams |
| Kodak Sodium Hydroxide (Caustic Soda) | 1-1/4 | ounces | 5 ounces | 37.5 grams |
| Kodak Potassium Bromide | 1 | ounce | 4 ounces | 30.0 grams |
| Water to make | 32 | ounces | 1 gallon | 1.0 liter |
| KODAK DEVELOPER D-19 | | | | |
| | Avoirdupois-U.S. Liquid | | | Metric |
| | Water, about 125°C (50°C) | 16 | ounces | 64 ounces |
| Kodak Elon Developing Agent | 30 | grains | 115 grains | 2.0 grams |
| Kodak Sodium Sulfite, desiccated | 3 | ounces | 12 ounces | 90.0 grams |
| Kodak Hydroquinone | 115 | grains | 30 grains 1 ounce | 8.0 grams |
| Kodak Sodium Carbonate, monohydrated | 1-3/4 | ounces | 7 ounces | 52.5 grams |
| Kodak Potassium Bromide | 75 | grains | 290 grains | 5.0 grams |
| Cold water to make | 32 | ounces | 1 gallon | 1.0 liter |

KODAK MICRODOL-X DEVELOPER

Kodak Microdol-X Developer is an excellent fine-grain developer unmatched for its ability to produce low graininess coupled with maximum sharpness of image detail. It has very little tendency to sludge when dissolved in hard water, and has no tendency to form scum on exhaustion, aeration, and replenishment. In addition to these advantages, Microdol-X Developer produces a very low fog level even with forced development of fine-grain films.

TABLE 2.- Developer Formulations (Concluded)

| ILFORD | | |
|--------------------------|-----------|--|
| ID-19 | | |
| Metol | 2.2 g | |
| Sodium sulphite, anhyd | 72 g | |
| Hydroquinone | 8.8 g | |
| Sodium carbonate, anhyd | 48 g | |
| Potassium bromide | 4 g | |
| Water to | 1 liter | |
| ILFORD ID-13 | | |
| PART A | | |
| Hydroquinone | 25 g | |
| Potassium Metabisulphite | 25 g | |
| Potassium Bromide | 25 g | |
| Water to make | 1.0 liter | |
| PART B | | |
| Potassium Hydroxide | 50 g | |
| Water to make | 1.0 liter | |

TABLE 3.- Effect of Developer Variation

| Film | Developer | Background Fog % Blackening | Exposure For 50% Blackening m Watt s cm ⁻² | |
|------|--------------------------|--------------------------------|--|--------------------|
| SC7 | D-19 3 minutes | 11 | 0.00145 | } Best |
| SC7 | D-19 6 minutes | 37 | 0.00115 | |
| SC7 | D-19 9 minutes | 55 | 0.00166 | } Excessive Fog |
| SC7 | D-19 12 minutes | 55 | 0.00145 | |
| SC7 | Microdol-X 30 minutes | 28 | 0.00290 | |
| SC7 | D-8 2 minutes | 24 | 0.00290 | |
| Q2 | D-19 3 minutes | 15 | 0.00640 | } Best |
| Q2 | D-19 6 minutes | 24 | 0.0050 | |
| Q2 | D-8 2 minutes | 11 | 0.0050 | |

TABLE 4. Smallest Demonstrated Detectable Signal, pA cm⁻²

| Ion | Energy | Ilford Q2 | Kodak SC7 |
|------------------|---------|-------------------------|-------------------------|
| H ⁺ | 500 eV | 5.0 pA cm ⁻² | 0.5 pA cm ⁻² |
| | 1000 eV | 1.0 pA cm ⁻² | 0.2 pA cm ⁻² |
| | 1300 eV | 0.6 pA cm ⁻² | 0.1 pA cm ⁻² |
| He ⁺⁺ | 750 eV | 5.0 pA cm ⁻² | 2.0 pA cm ⁻² |
| | 1650 eV | 2.0 pA cm ⁻² | 1.0 pA cm ⁻² |
| | 2500 eV | 1.0 pA cm ⁻² | 0.5 pA cm ⁻² |
| N ⁺ | 6 keV | 0.5 pA cm ⁻² | 0.3 pA cm ⁻² |
| | 8 keV | 0.5 pA cm ⁻² | 0.2 pA cm ⁻² |
| | 10 keV | 0.5 pA cm ⁻² | 0.1 pA cm ⁻² |

Finally the effect of secondary ions can greatly effect the minimum detectable signal when a weak line is being studied that is adjacent to a line several orders of magnitude more intense. This phenomena causes a tail on the high mass side of the intense line. The effect becomes noticeable at exposures approximately 10 times greater than that required for 95 percent blackening, for this reason it became apparent on only a few patches of the present study. Cavard has studied it in detail and has devised some special developers which minimize the problem. The overall sensitivity is, however, degraded by using these developers. An alternate approach to this problem is presented by Clegy¹⁴ who has experimented with shields which prevent the intense lines from reaching the plate.

CONCLUSIONS

The Ilford Q2 and Kodak SC7 have a sensitivity to light ions that greatly exceeds the sensitivity for heavier ions of the same energy, making these emulsions excellent detectors for the solar wind plasma. For ions traveling at the same velocity with an energy of 1 keV per M/Q, the exposure required for fifty percent blackening is approximately:

$$SC7 = 9.5 \times 10^{-8} \sqrt{M} \text{ cm}^2 \text{ per ion}$$

$$Q2 = 1.3 \times 10^{-8} \sqrt{M} \text{ cm}^2 \text{ per ion}$$

independent of the ion charge state.

This relation should be considered a rough estimate only, because of the limited number of ions and charge states included in this study.

¹⁴Reference 14, p. 83. This reference will be found in the bibliography.

APPENDIX A
ILLUSTRATIONS

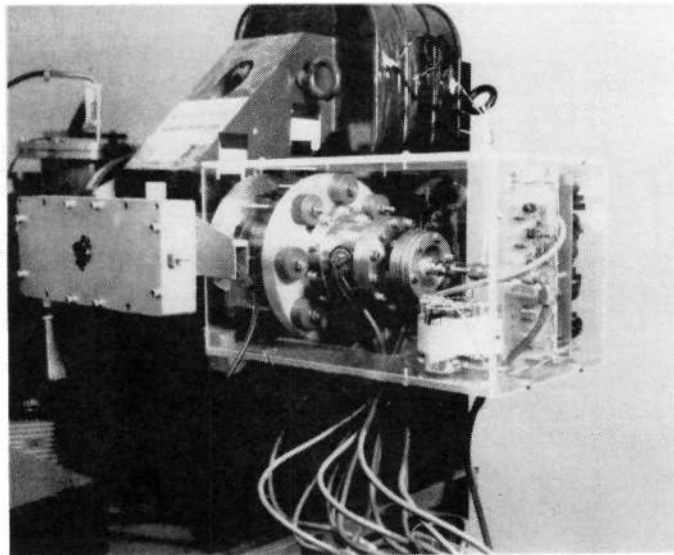


FIGURE 1.- Mass Analyzer

The Mass Analyzer used to generate the ions used in the study. The ion source, insulated and shielded for voltages to 10 kV is on the right. The removable film cassette is on the left. The yoke and coils of the 0-7 k gauss electromagnet also form the supporting structure.

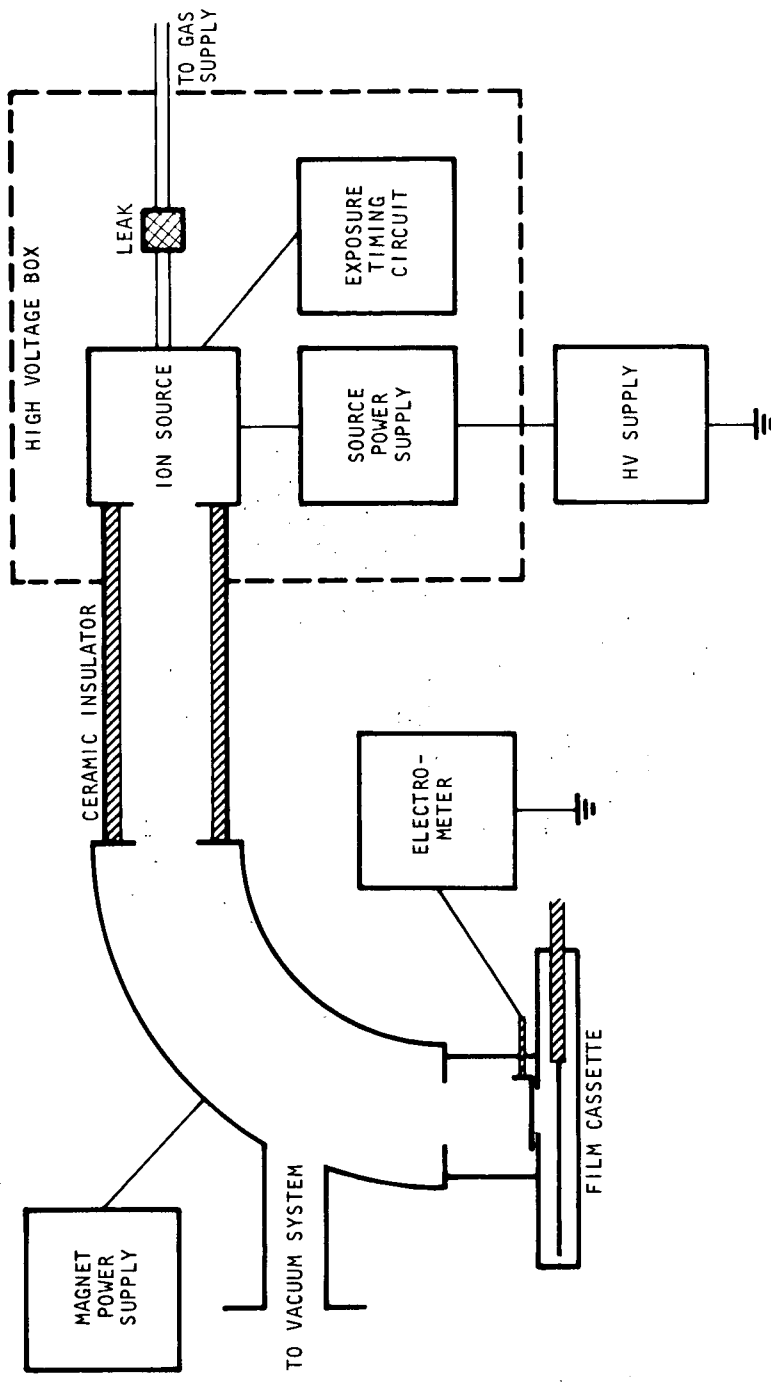


FIGURE 2.- Block Diagram of Source, Analyzer, Cassette and Power Supplies

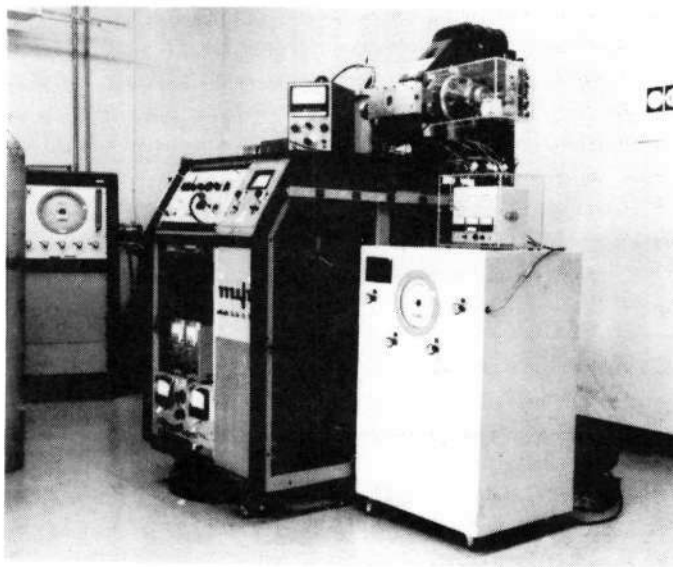


FIGURE 3.- Overall View of Mass Analyzer
and Support Equipment

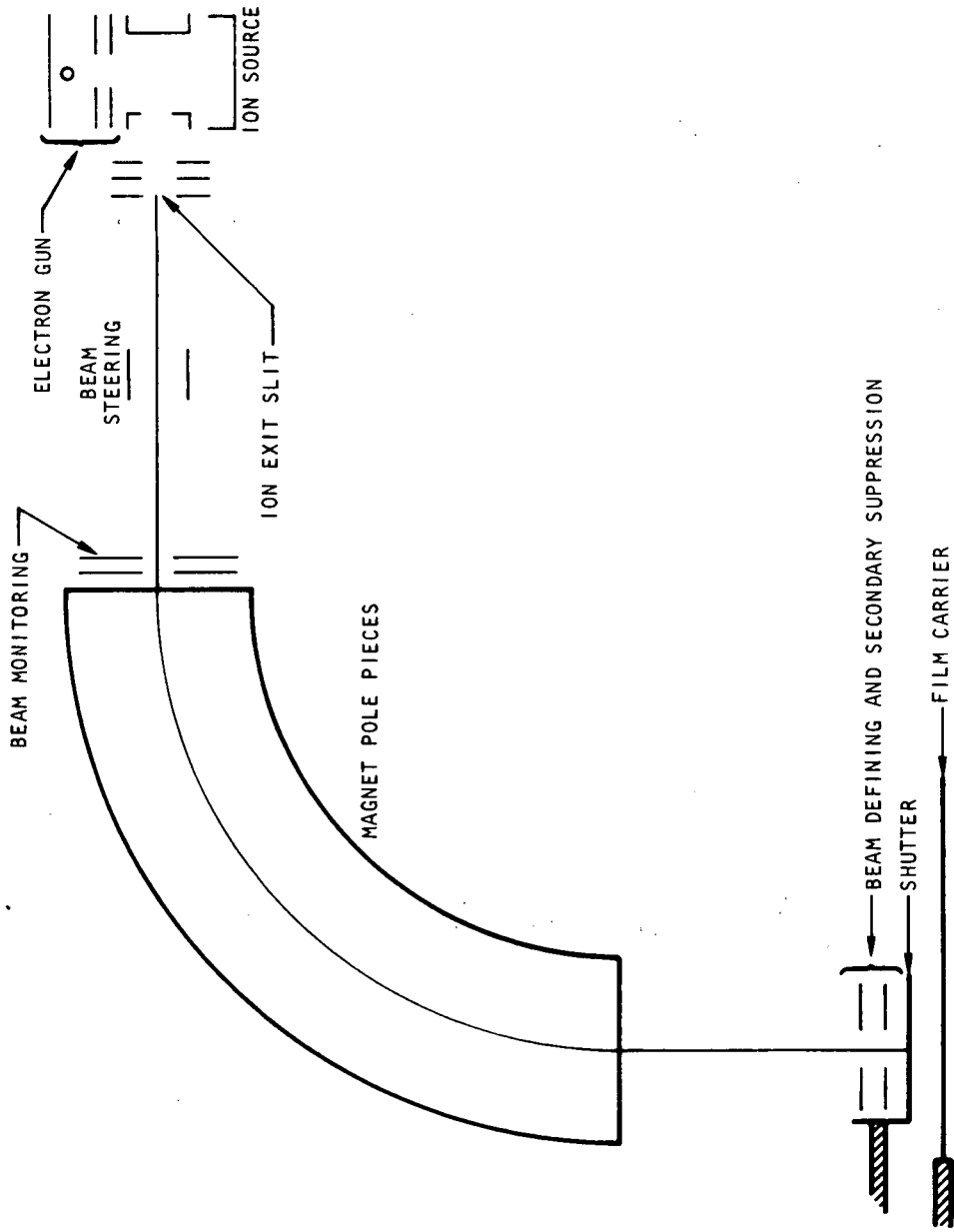


FIGURE 4.- Schematic of Electrode Arrangement of the Ion Source, Mass Analyzer, and Cassette

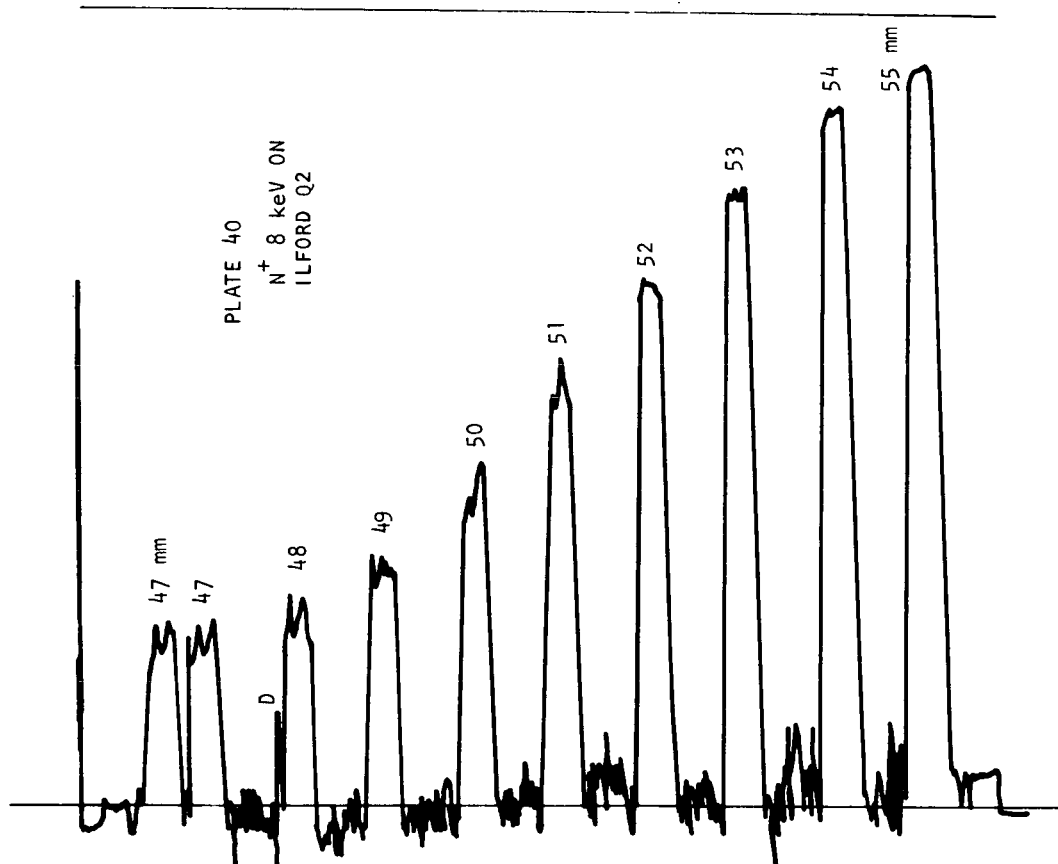


FIGURE 5.- A Typical Densitometer Trace Over a Set of Patches. The Exposure Time Varies by x2 From One Patch to the Next

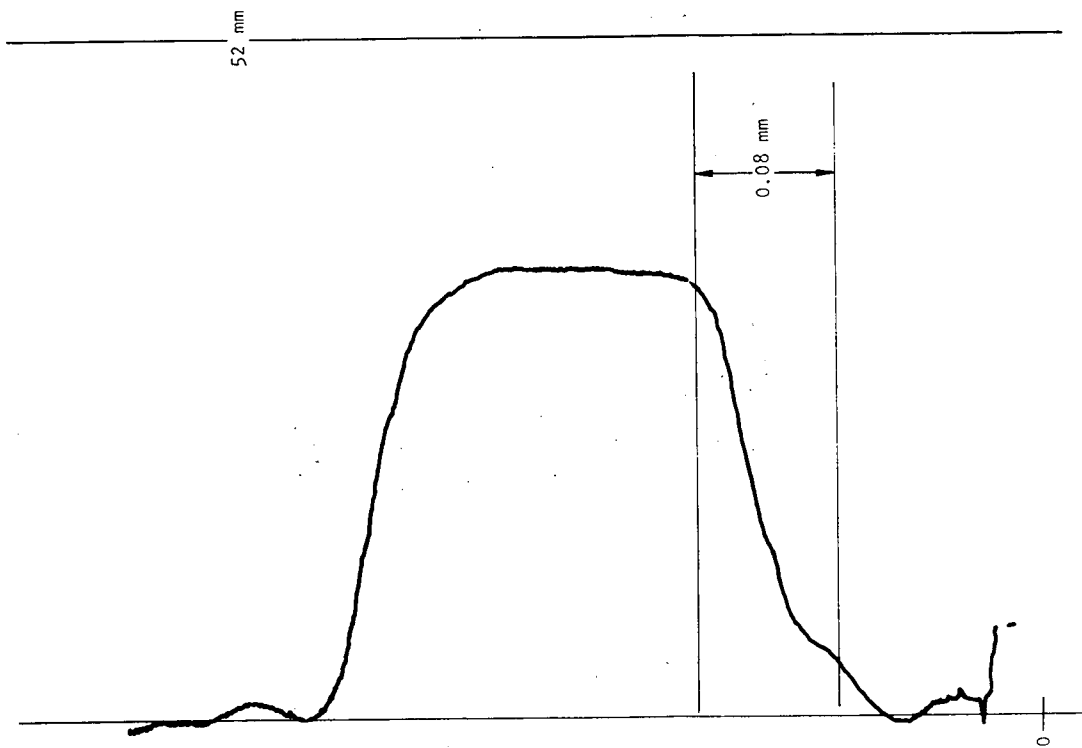


FIGURE 6.- A Detailed Trace of a Single Patch on the Densitometer, Illustrating Typical Resolution and Uniformity

Reproduced from
best available copy.

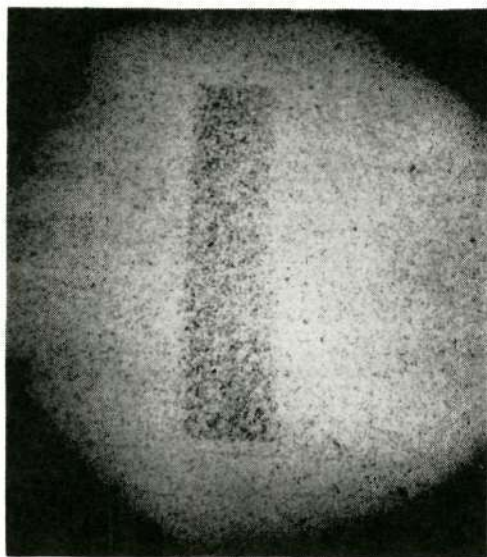


FIGURE 7.- A Typical Patch of Very Light Density.
 H^+ Ions at 900 eV on Kodak SC7. 0.78 pC cm^{-2}
Exposure. 33% Black.

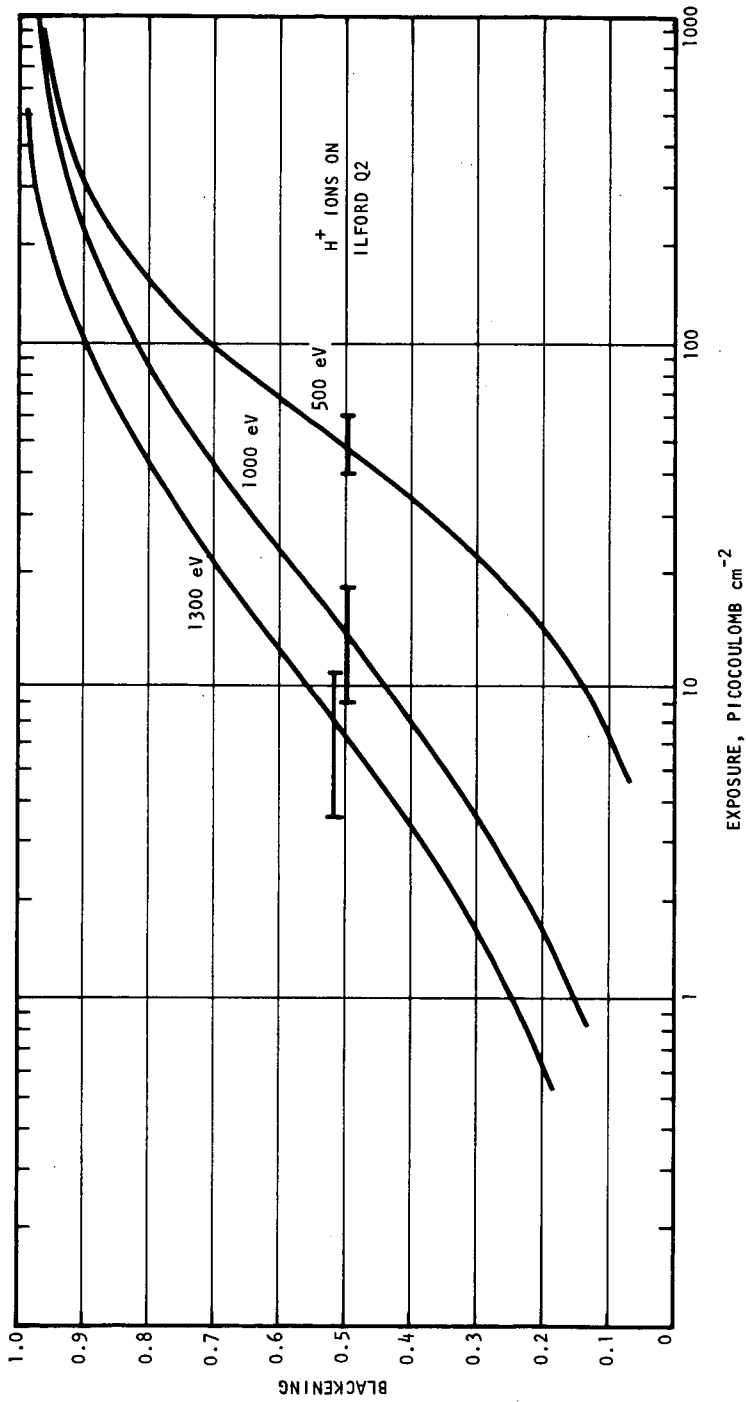


FIGURE 8.- H⁺ Ilford

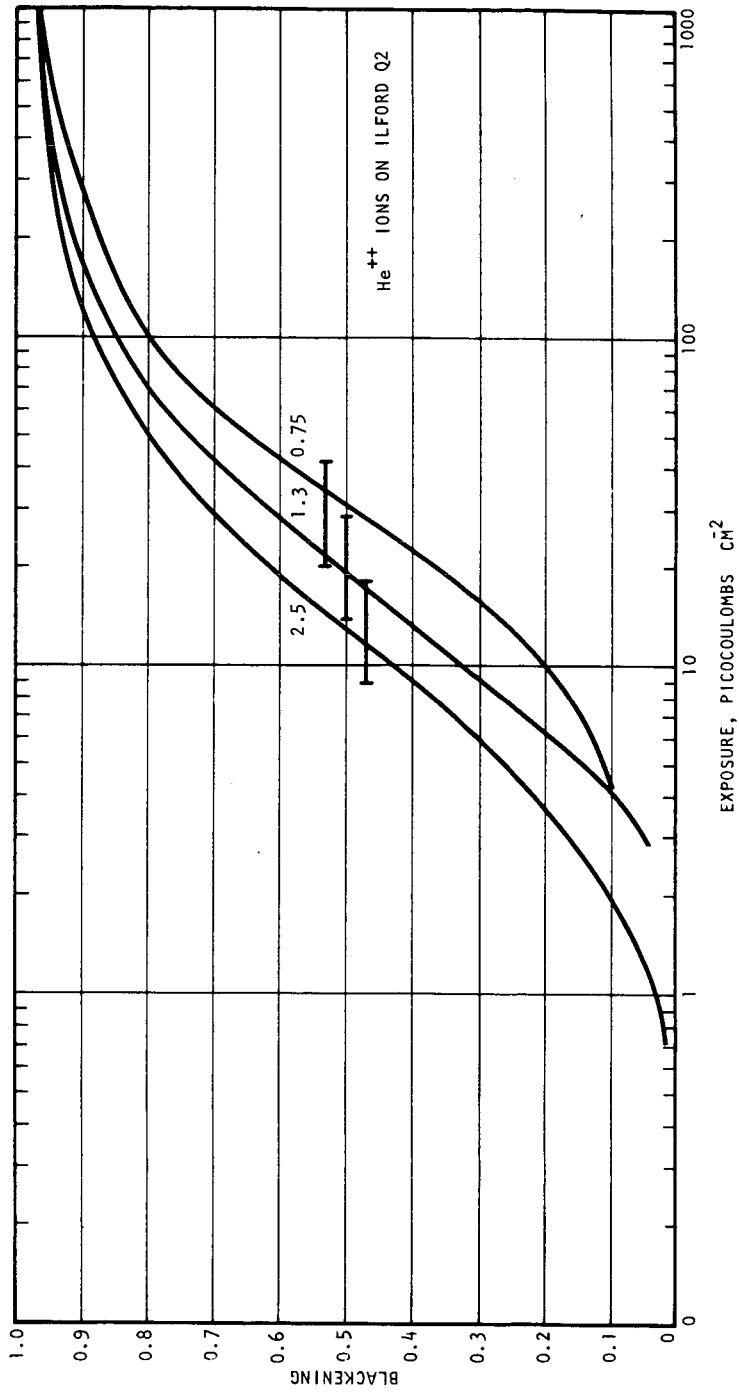


FIGURE 9.- He⁺⁺ Ilford

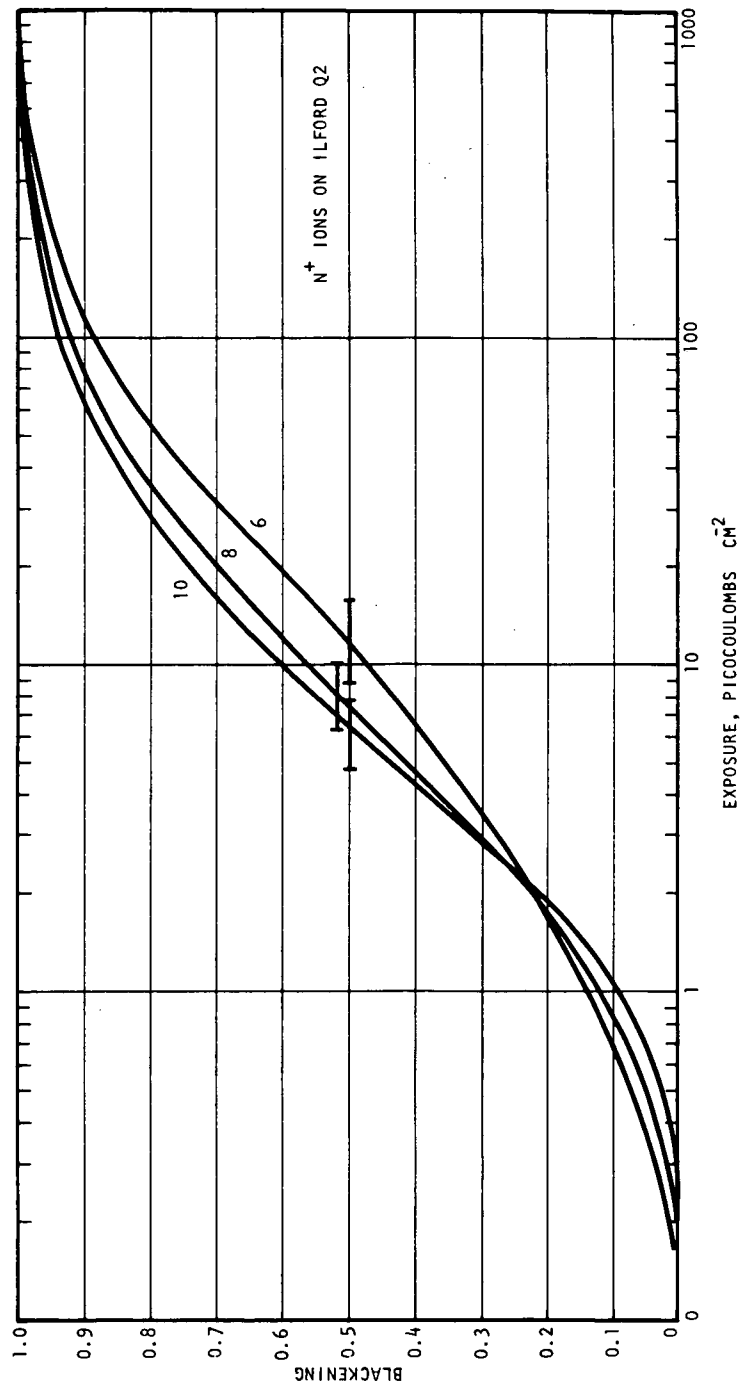


FIGURE 10.- N⁺ Ilford

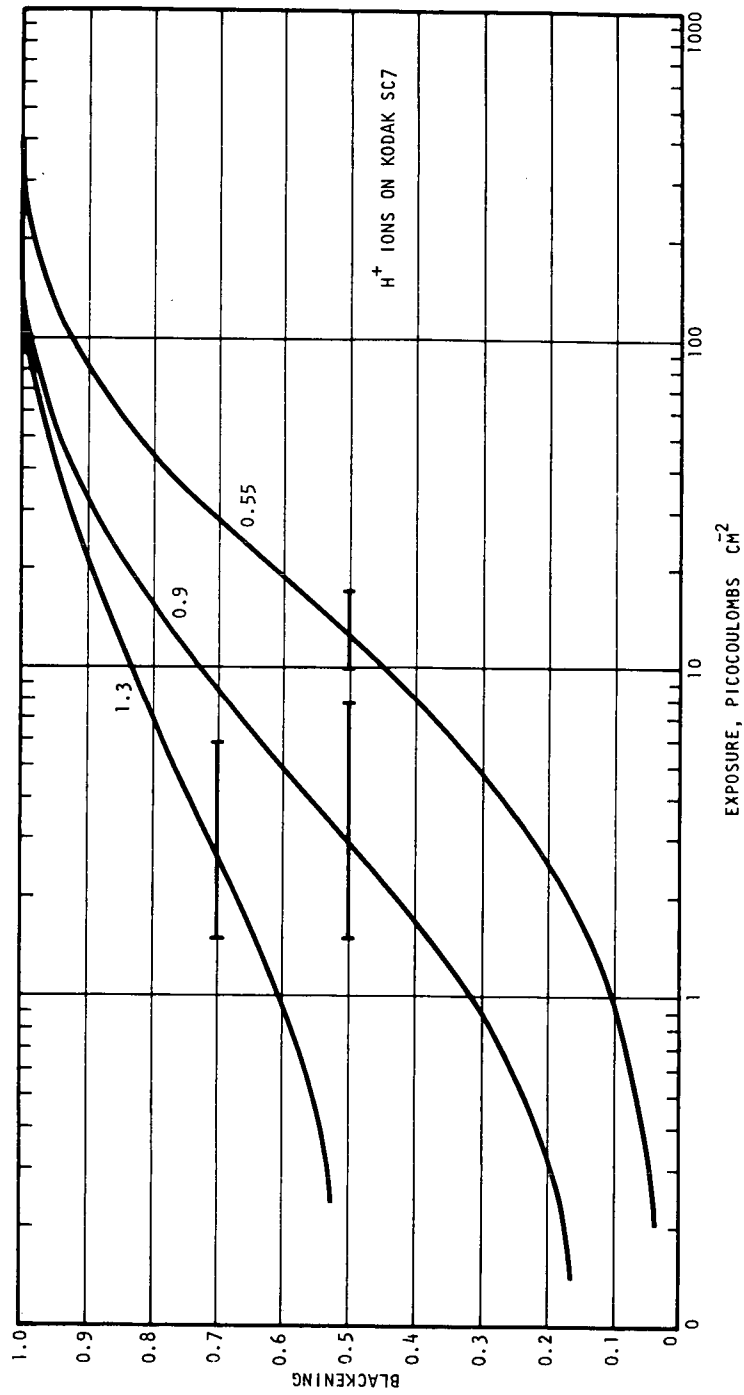


FIGURE 11.- H⁺ Kodak

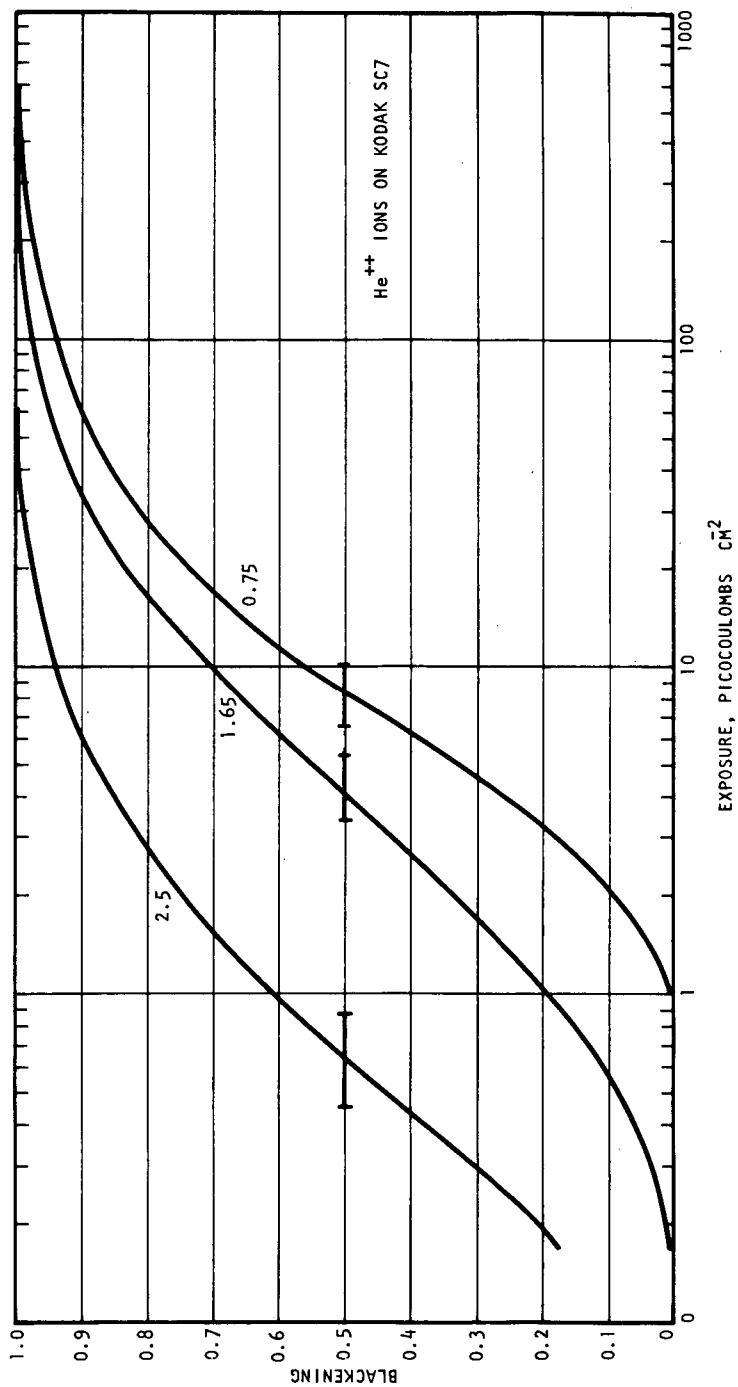


FIGURE 12.- He⁺⁺ Kodak

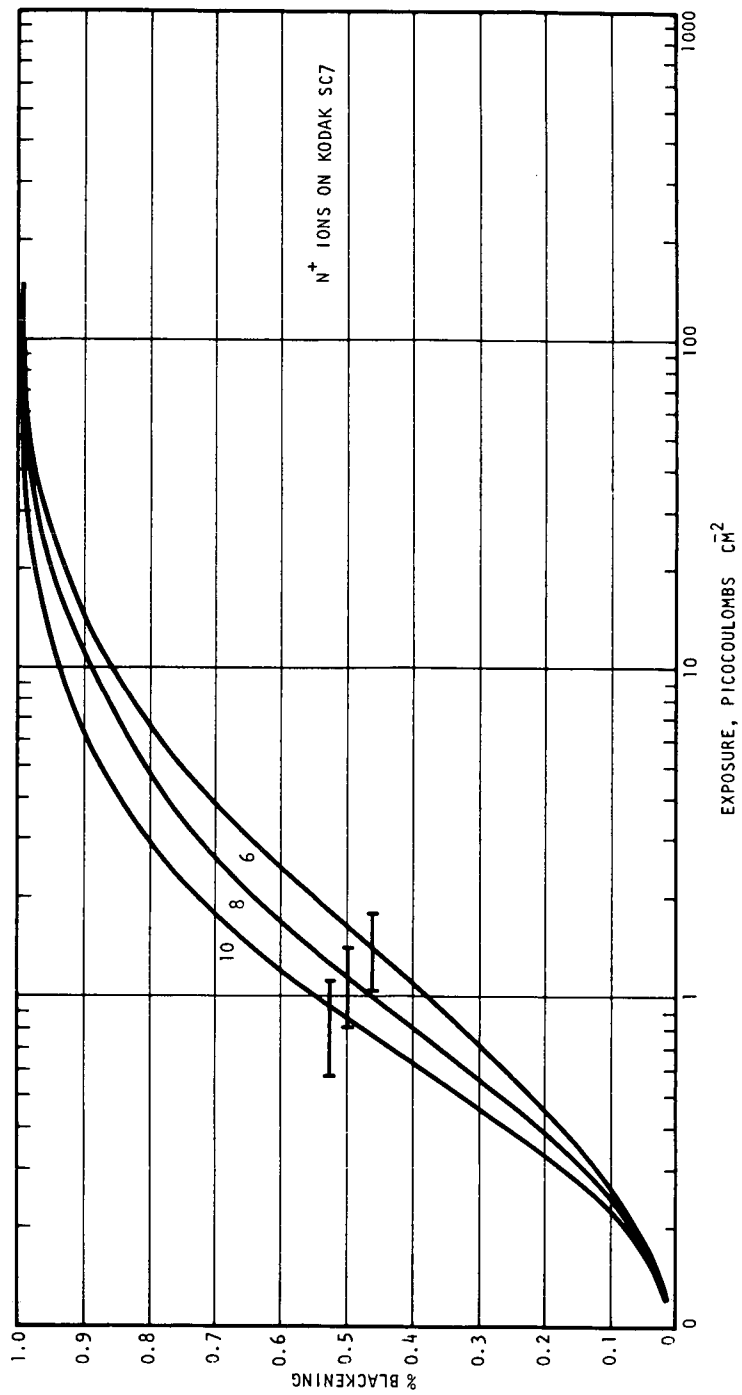


FIGURE 13.- N⁺ Kodak

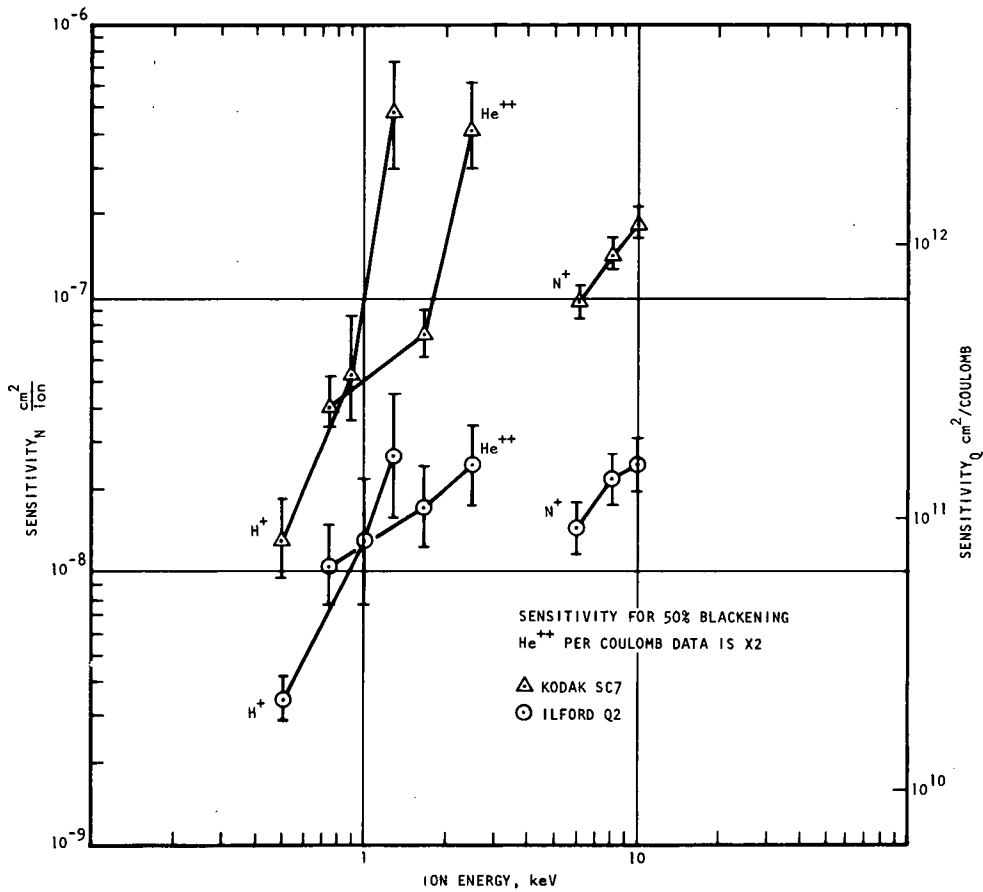


FIGURE 14.- Sensitivity of Ilford Q2 and Kodak SC7 as Functions of Energy for Various Ions. He^{++} Data is x2.

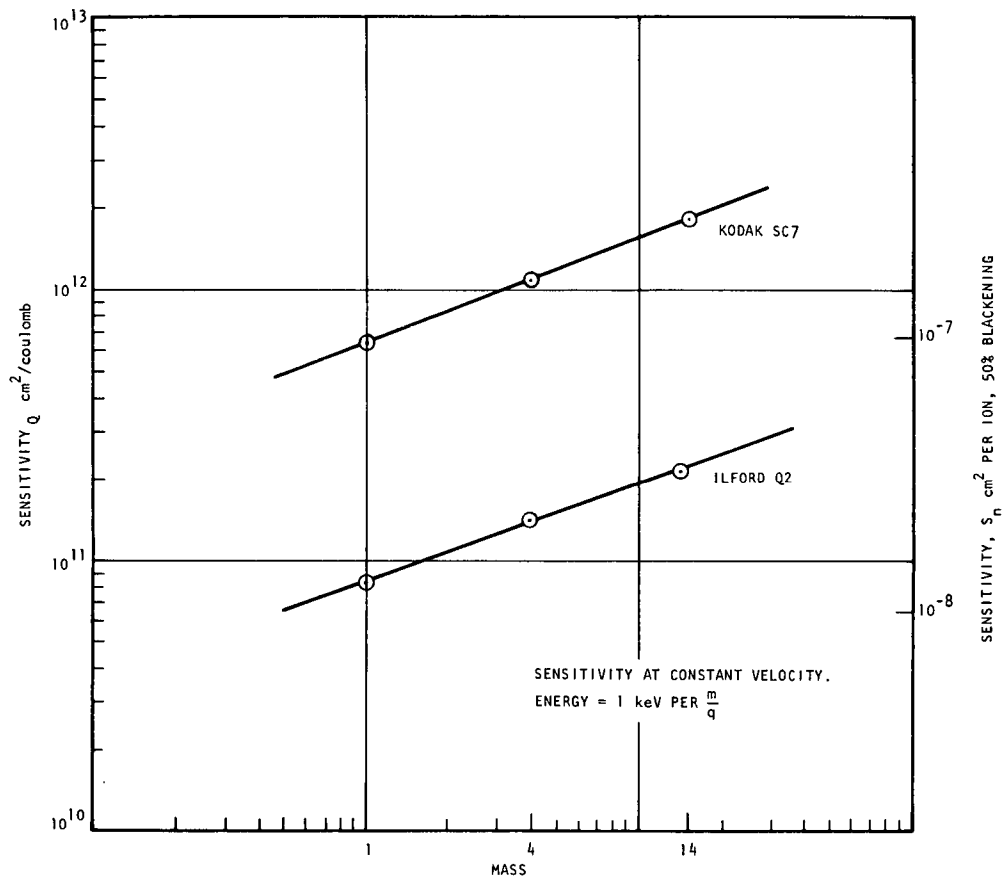


FIGURE 15.- Sensitivity of Ilford Q2 and Kodak SC7 as Function of Mass. He⁺⁺ Data is x2.

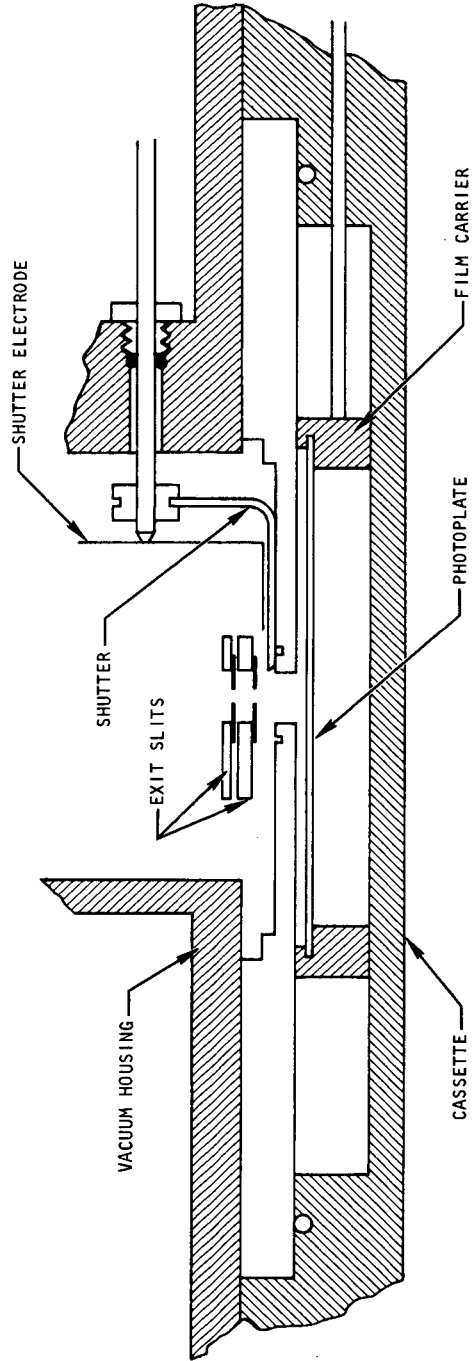


FIGURE 16. Detail of the Exit Slits, Cassette, and Film Plate Holder

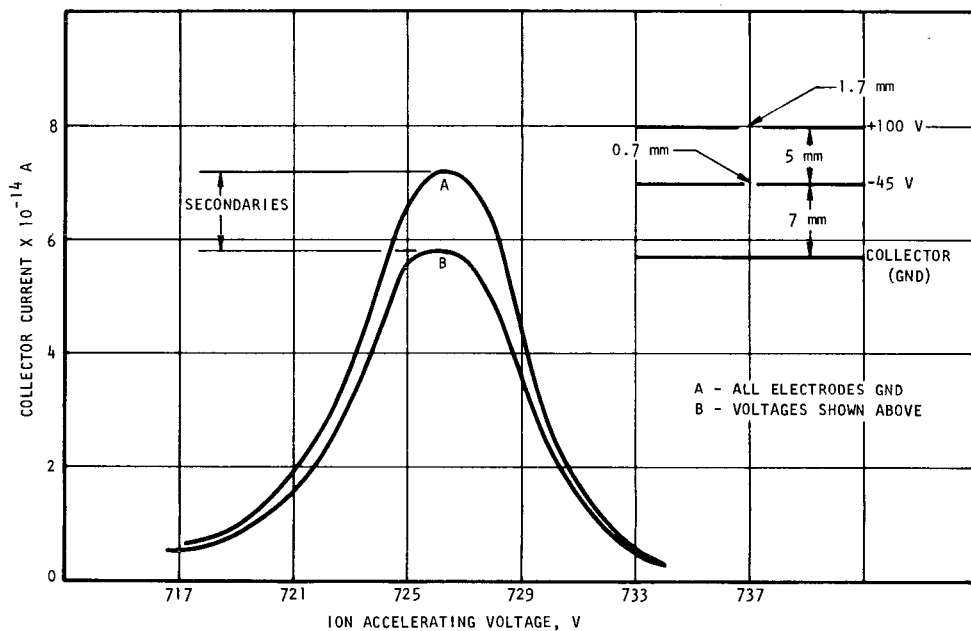


FIGURE 17.- Collector Current as N_2^+ Beam is Swept Past Exit Slits by Varying the Accelerating Voltage. The Inset Schematic Shows Slit Dimensions and Spacings. The Difference Between Curves A and B is the Contribution Due to Secondaries.

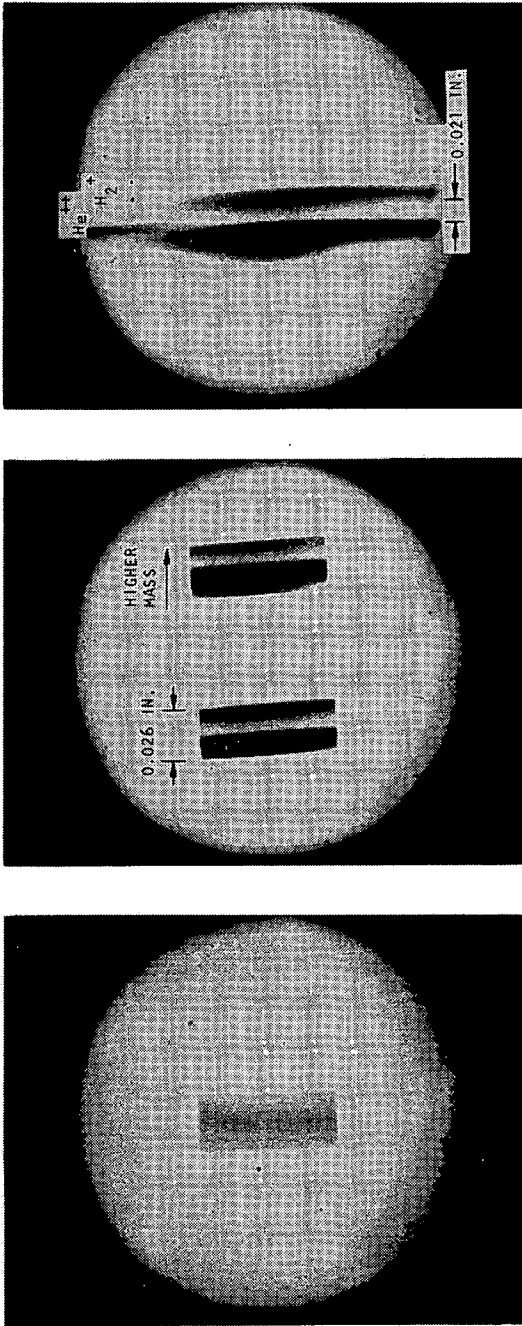


FIGURE 18.- Exposures of Ilford Q2 Plates to the He^{++} - H_2^+ Doublet

1. N_2^+ showing beam width and sharpness.
2. He^{++} - H_2^+ . Two images. The accelerating voltage was increased by 5 V and the plate moved for the right hand image, so that the patch is moved with respect to the slit.
3. He^{++} - H_2^+ with exit slits removed showing entire beam shape.

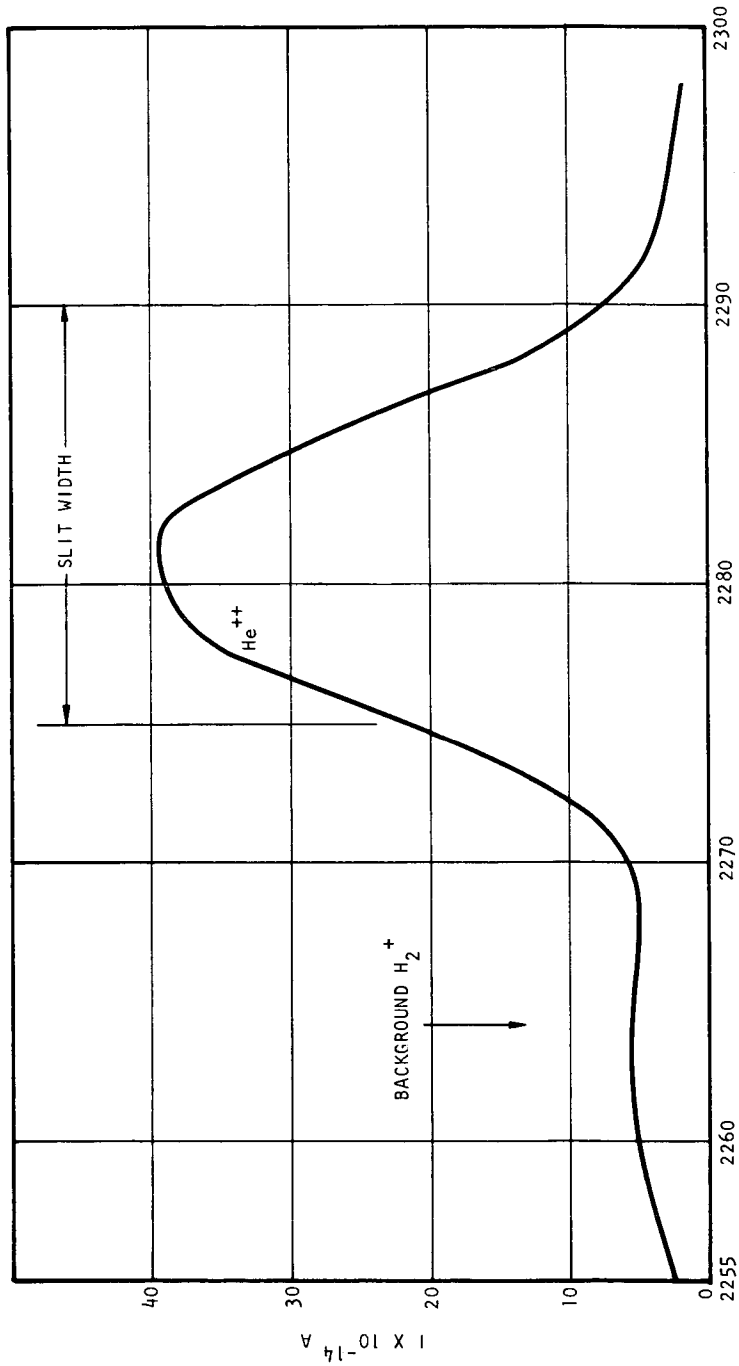
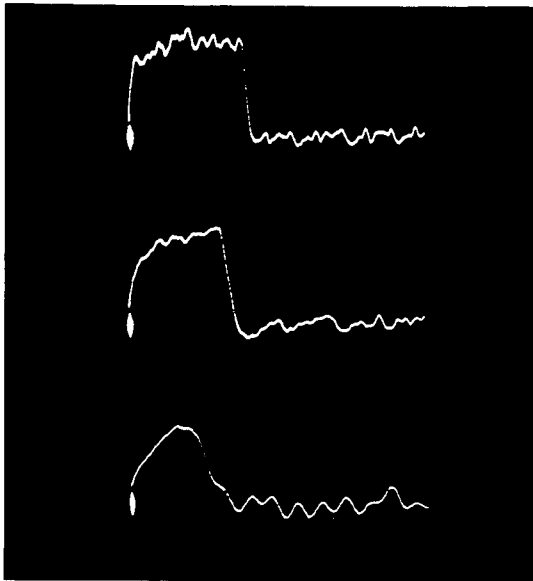


FIGURE 19.- Trace of the Ion Current Due to the $\text{He}^{++} - \text{H}_2^+$ Doublet as the Beams are Swept by 0.012 Inch Exit Slit by Varying Accelerating Voltage.



50 MILLISECONDS PULSE
X = 10 MSEC/DIV

20 MILLISECOND PULSE
X = 5 MSEC/DIV

5 MILLISECOND PULSE
X = 2 MSEC/DIV

FIGURE 20.- Typical Oscilloscope Traces of the Pulsed Ion Beam.
 N_2^+ Ions Amplified by the Keithley 610C Electrometers.
Resolution is Limited by Electrometer Response.

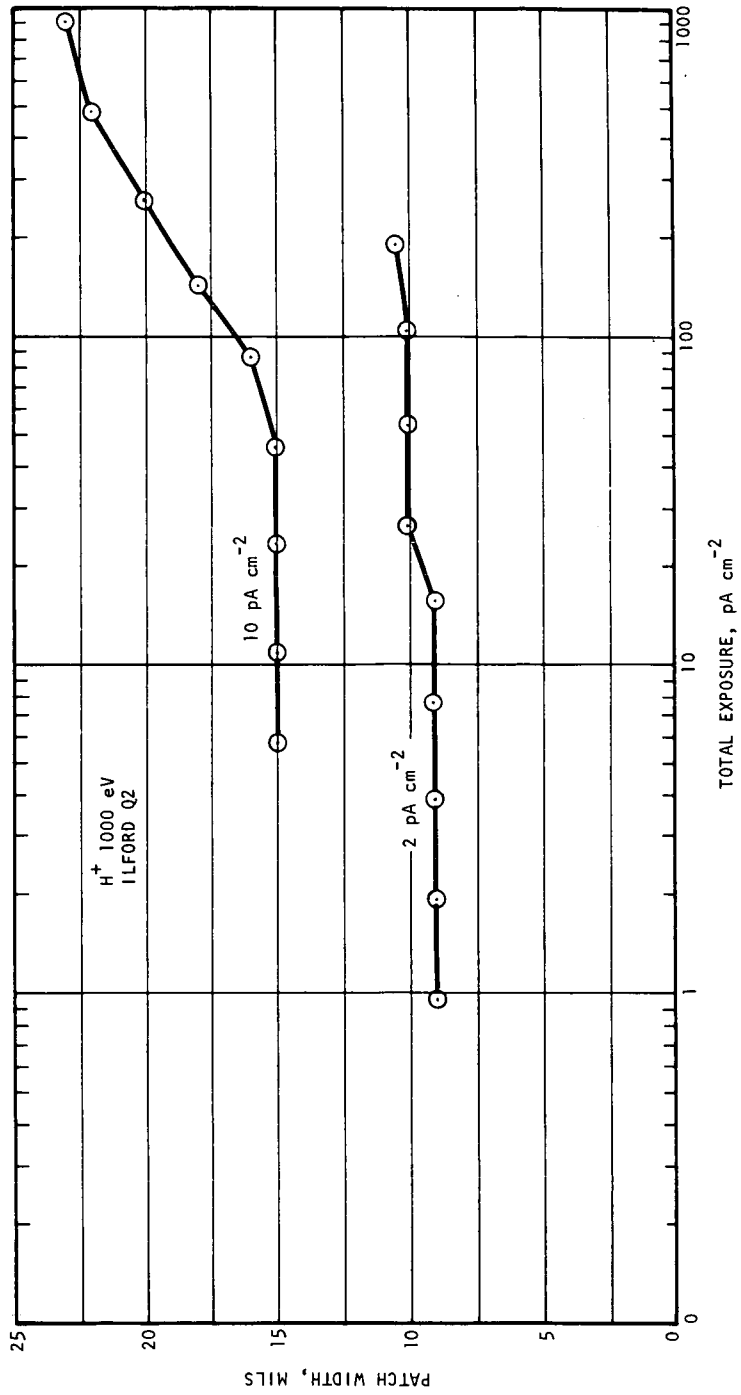


FIGURE 21.- Patch Width Spreading at Increased Current Levels
 Probably due to Surface Charging of the Insulating Emulsion

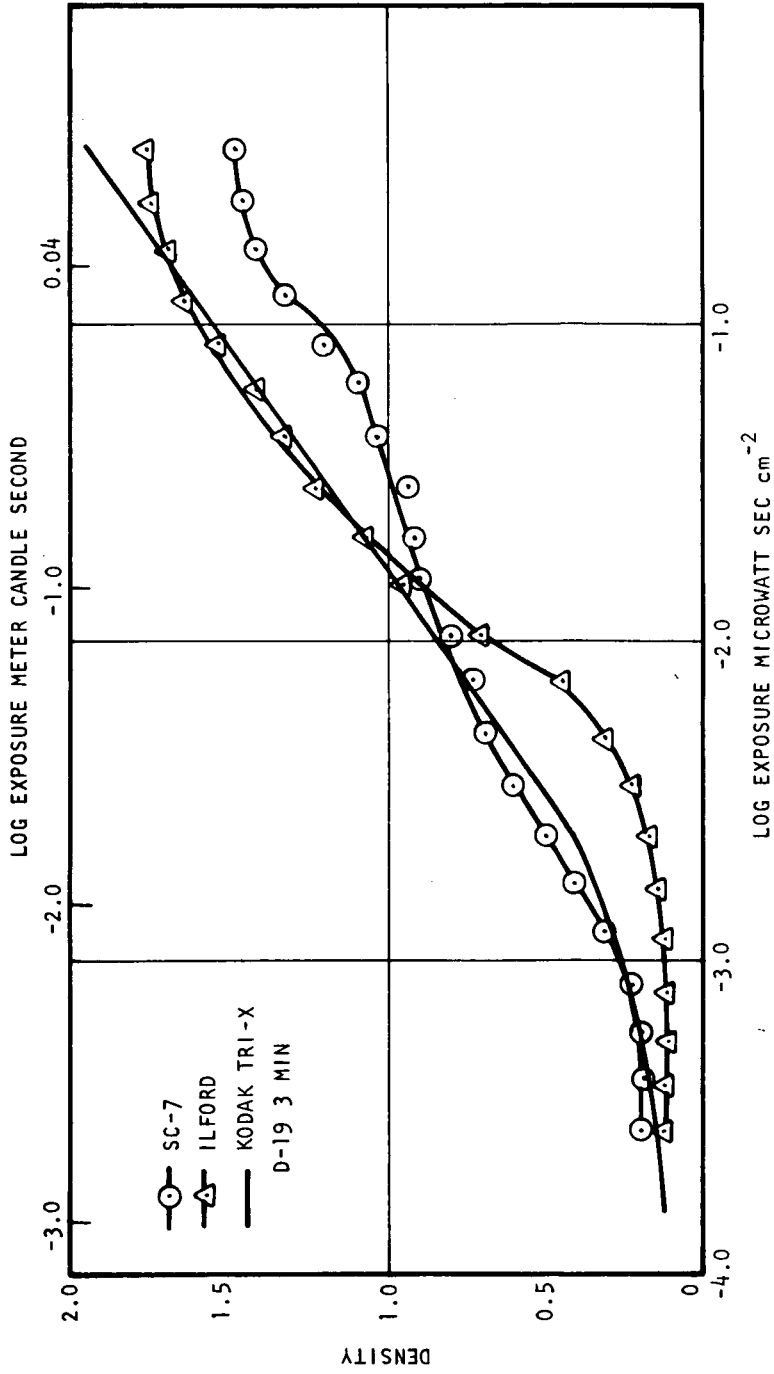


FIGURE 22.- Sensitivity of Ilford Q2 and Kodak SC7 to Simulated Visible Solar Radiation. Kodak Tri-X is Included for Comparison.

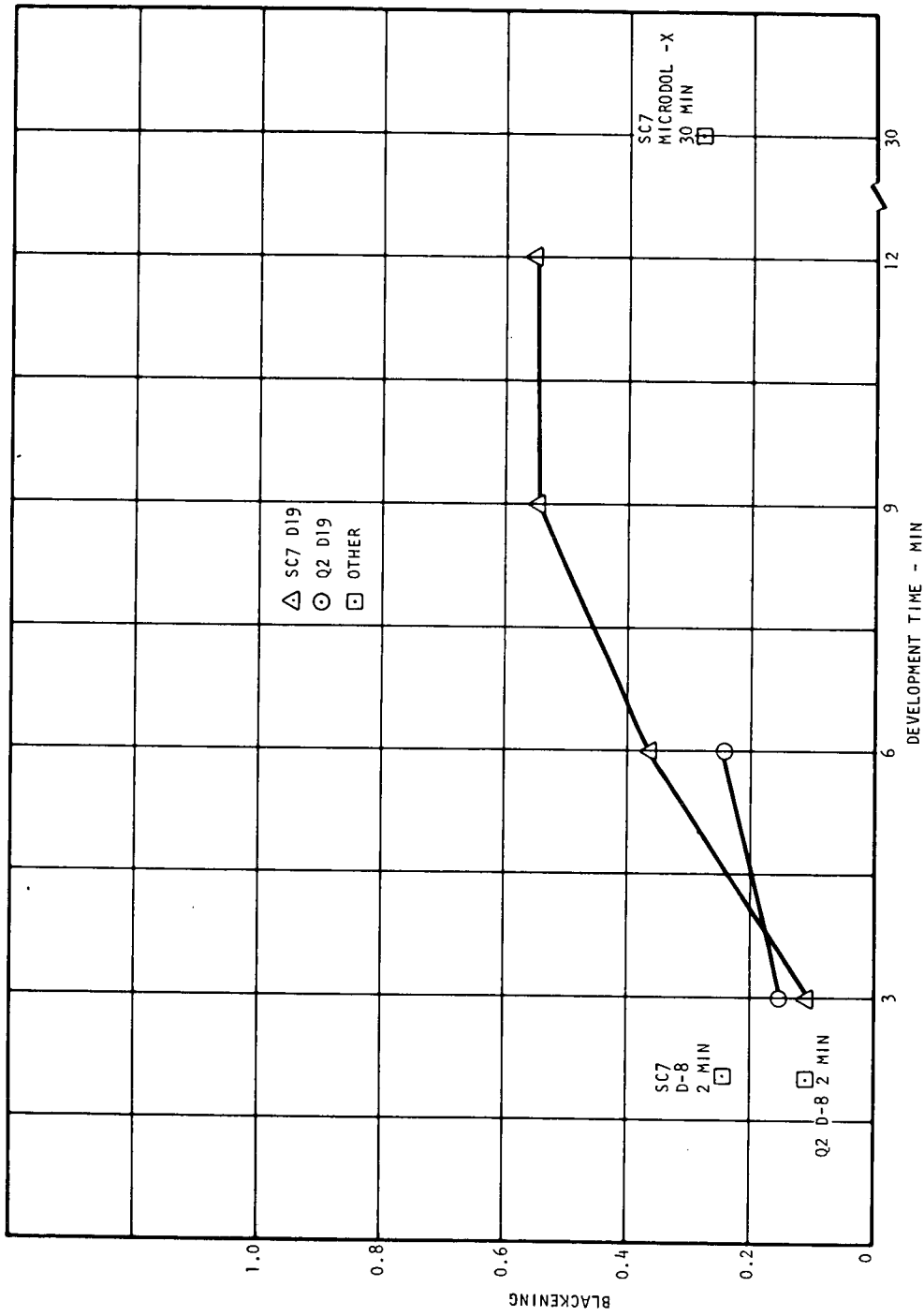


FIGURE 23.- Background Fog Level With Various Developers and Times

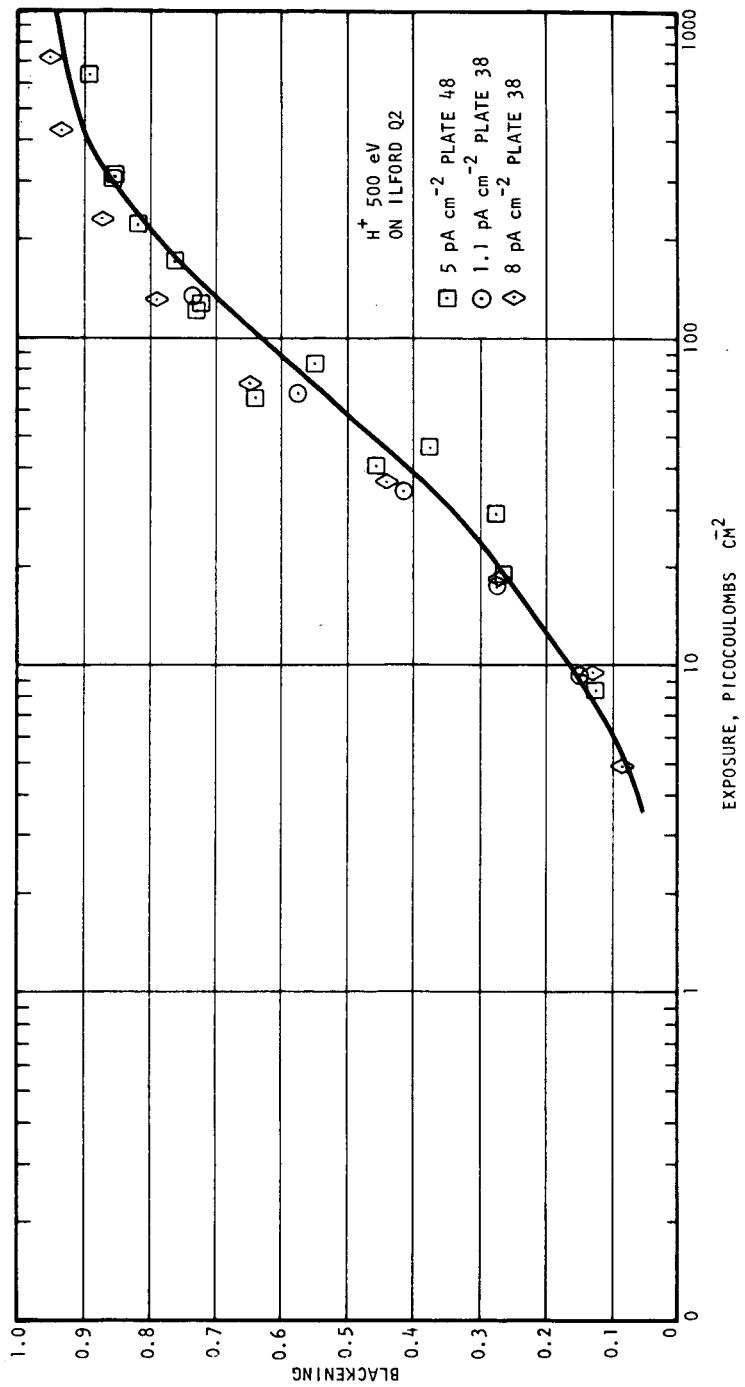


FIGURE 24.- H^+ Ilford (500 eV)

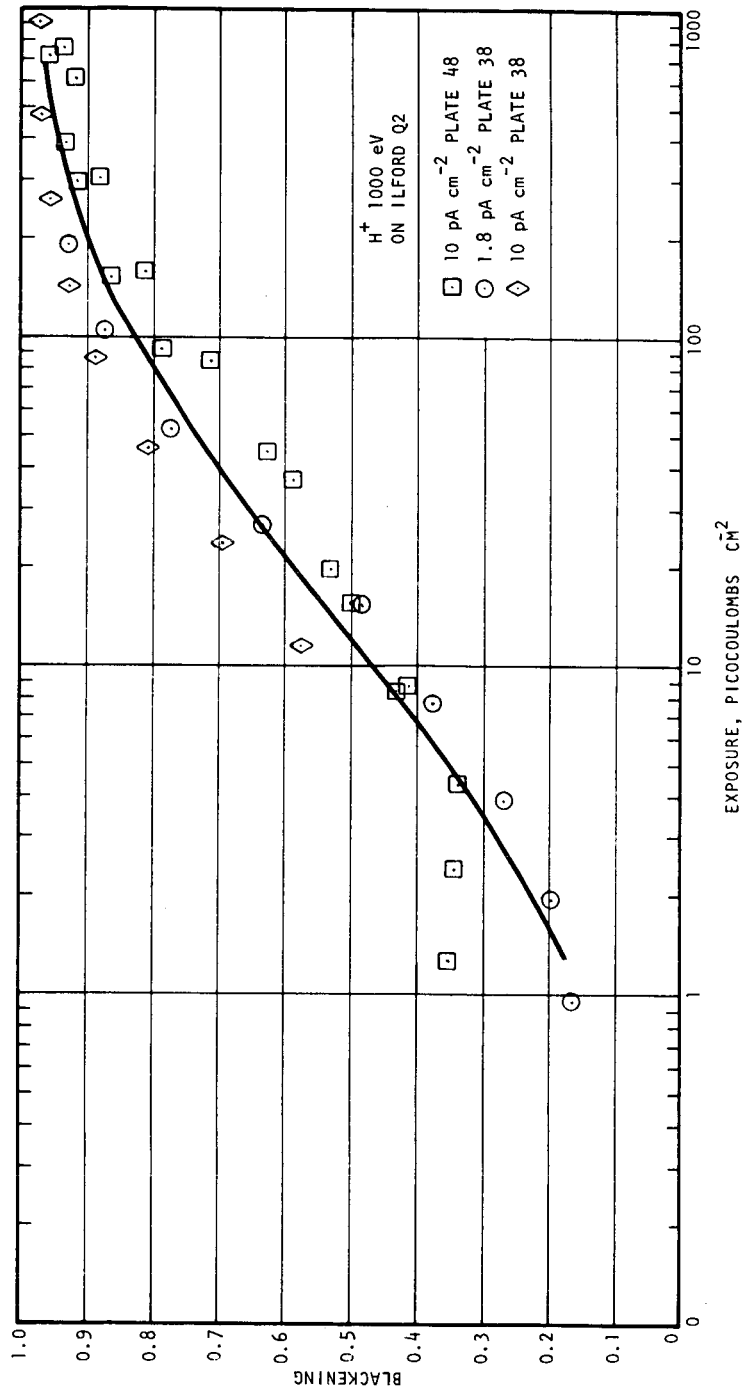


FIGURE 25.- H^+ Ilford (1000 eV)

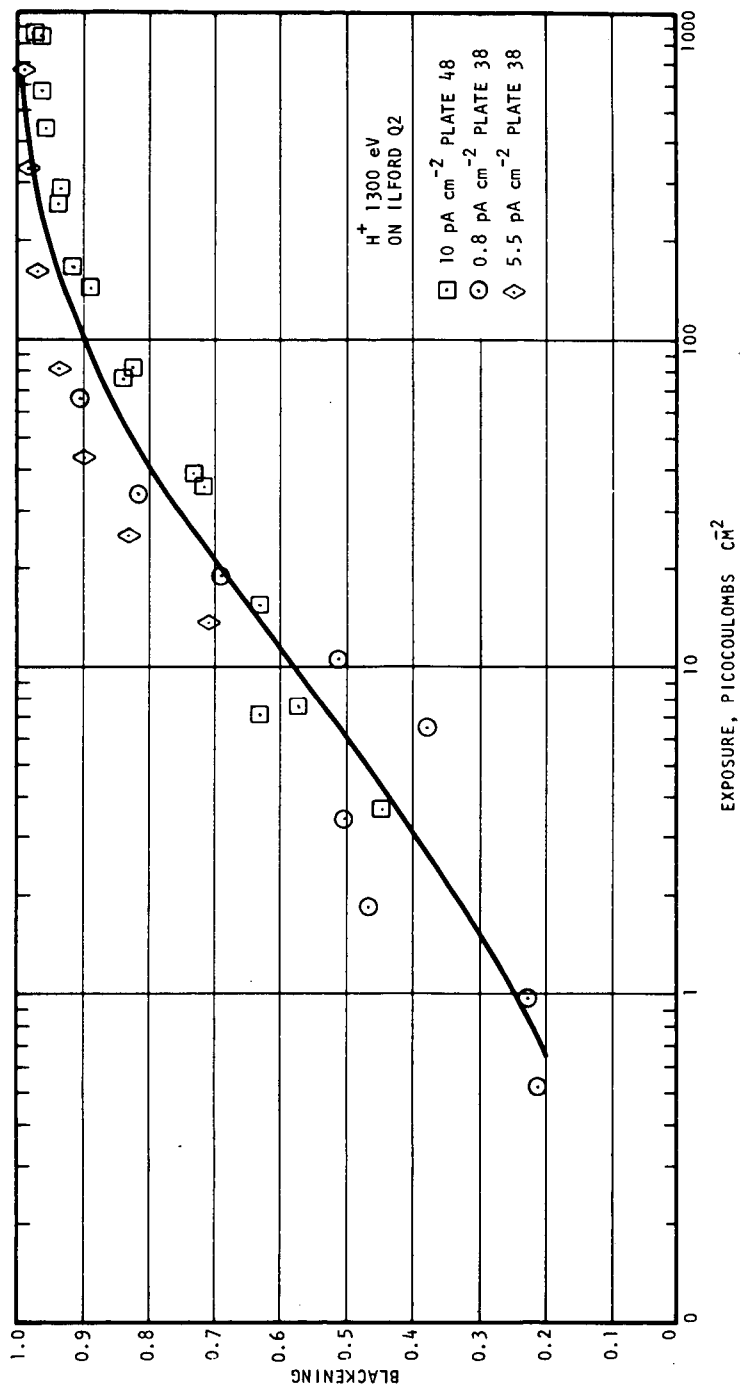


FIGURE 26.- H^+ Ilford (1300 eV)

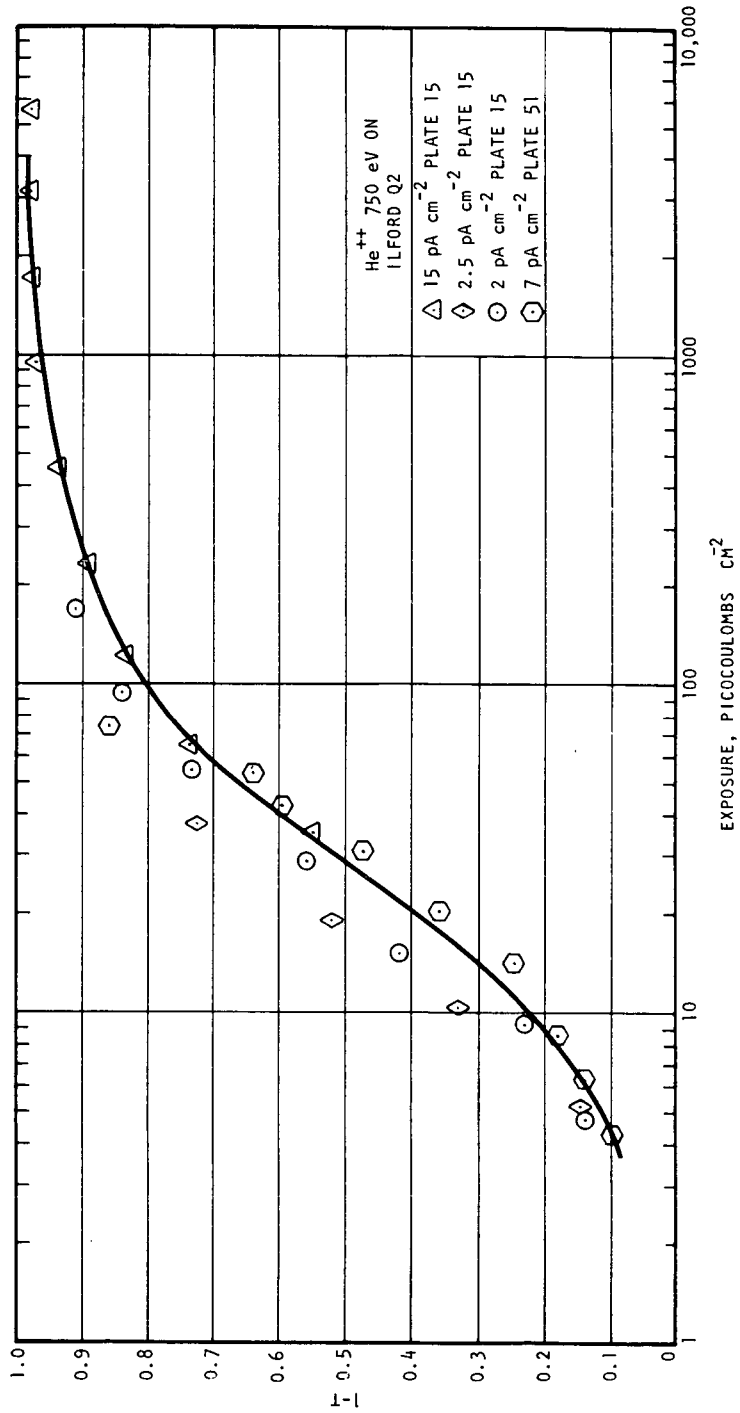


FIGURE 27.- He^{++} ILford (750 eV)

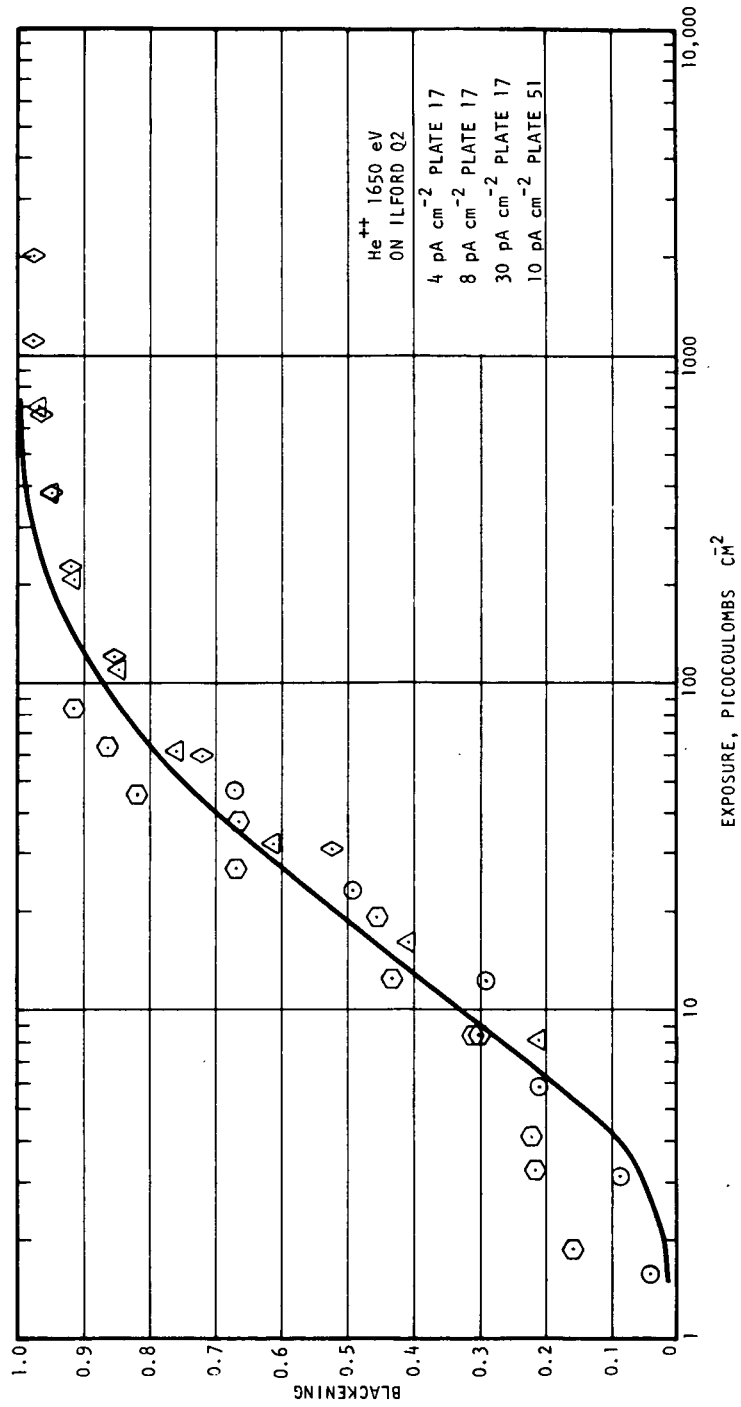


FIGURE 28.- He⁺⁺ Ilford (1650 eV)

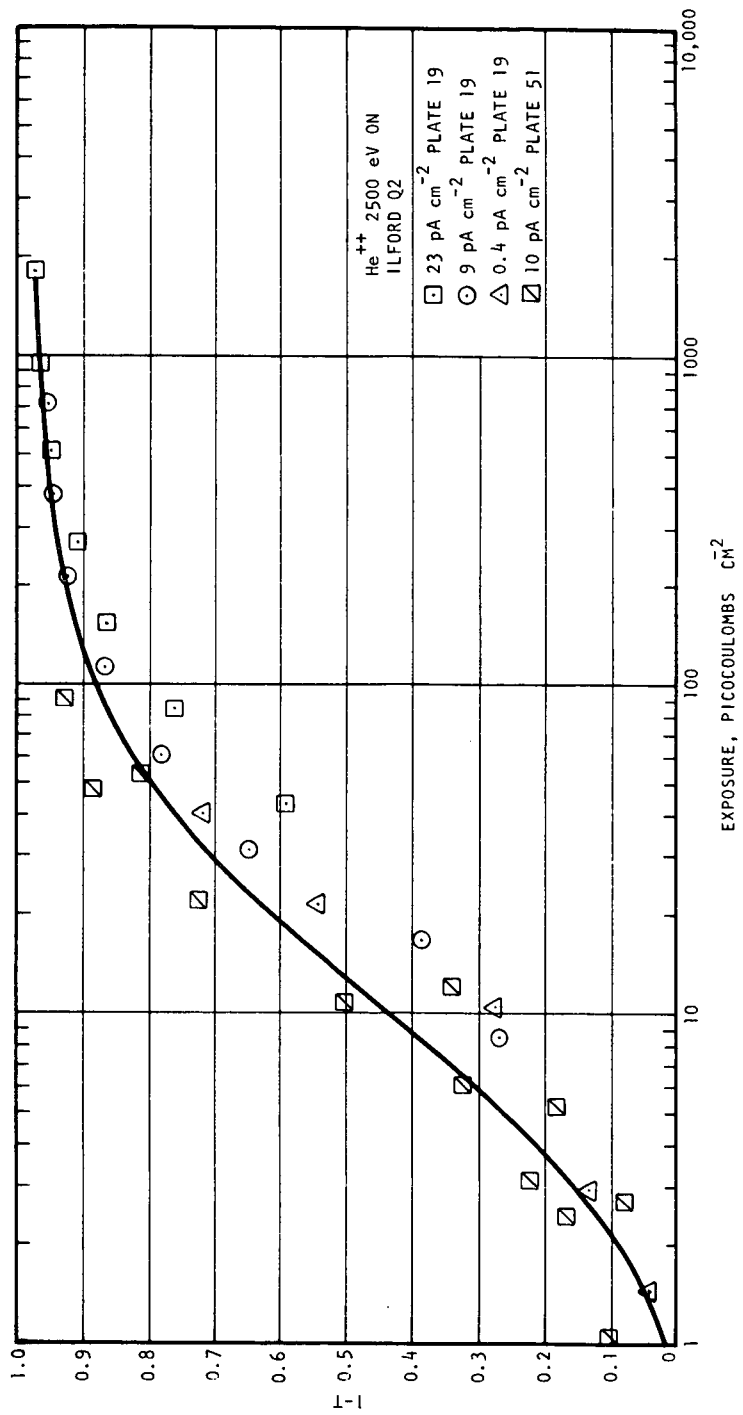


FIGURE 29.-- He^{++} Ilford (2500 eV)

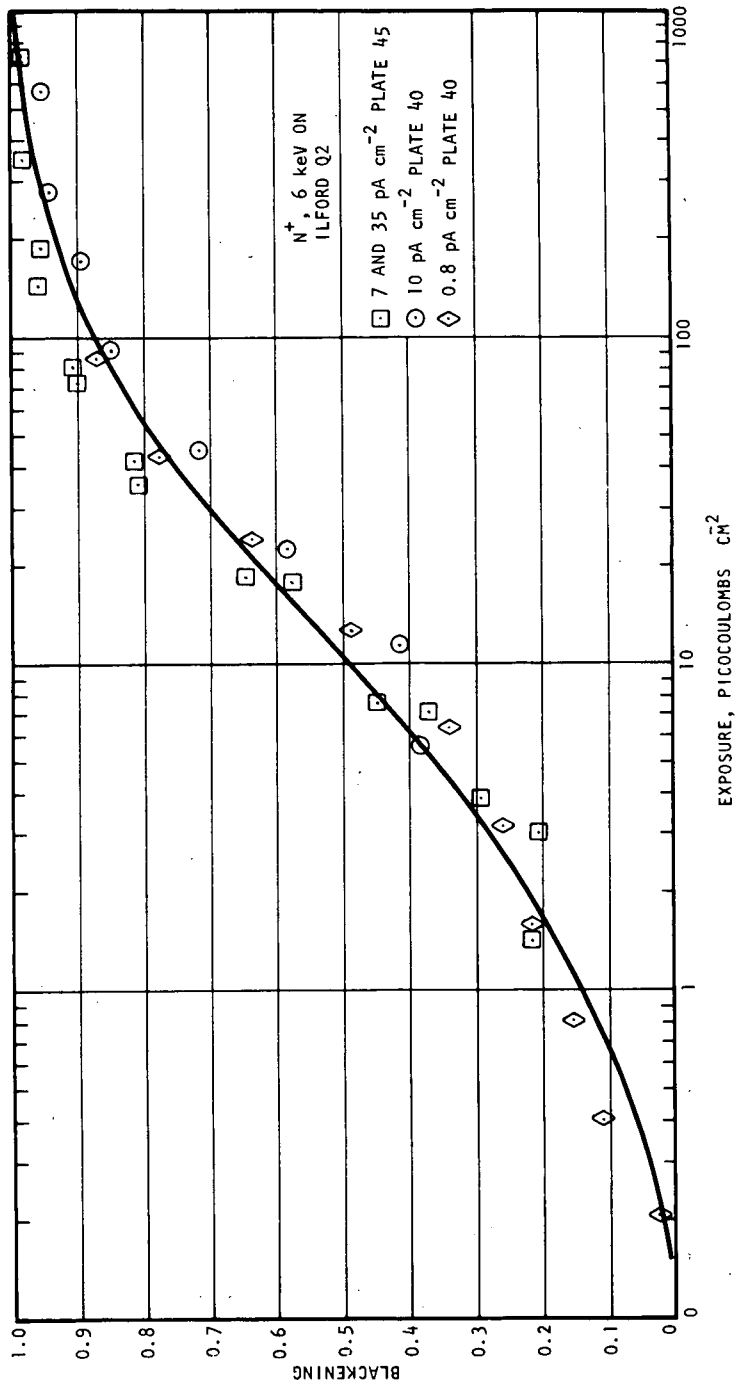


FIGURE 30.- N^+ Ilford (6 keV)

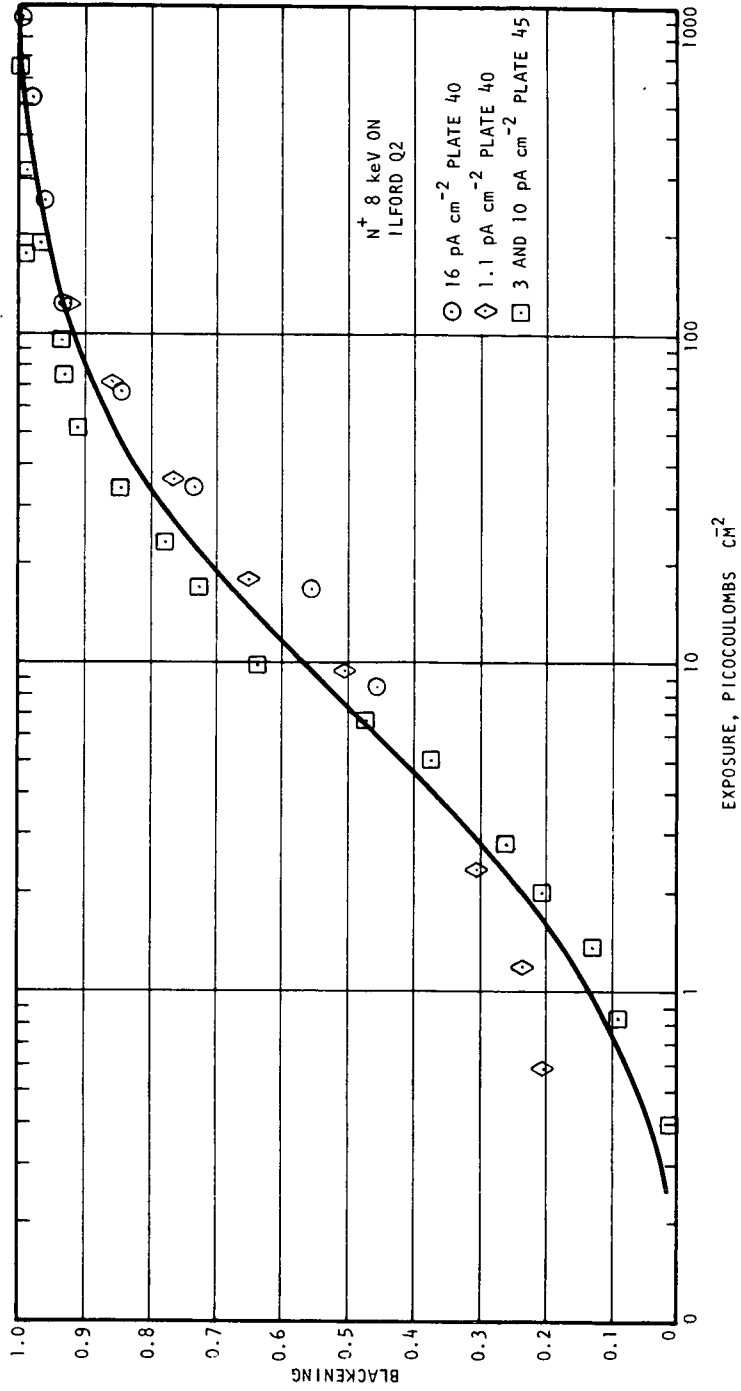


FIGURE 31.- N^+ Ilford (8 keV)

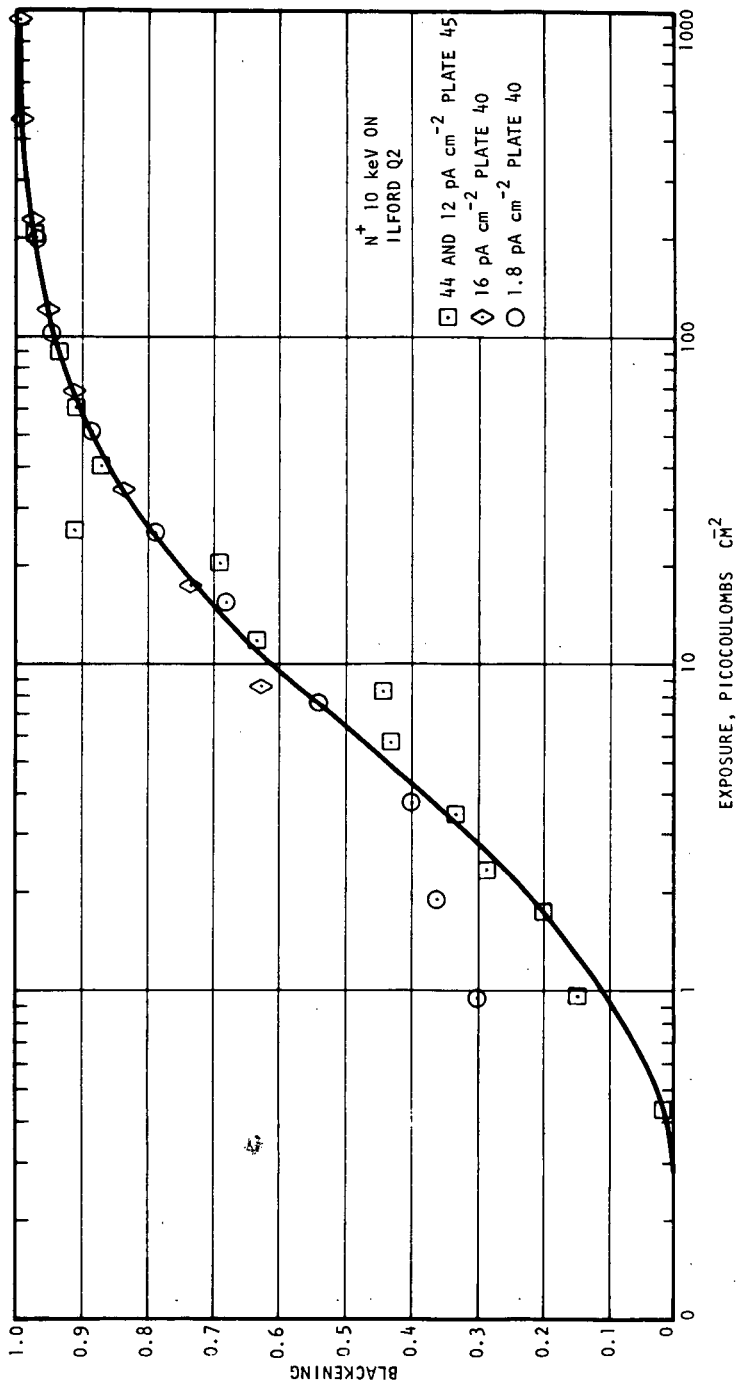


FIGURE 32.- N⁺ Ilford (10 keV)

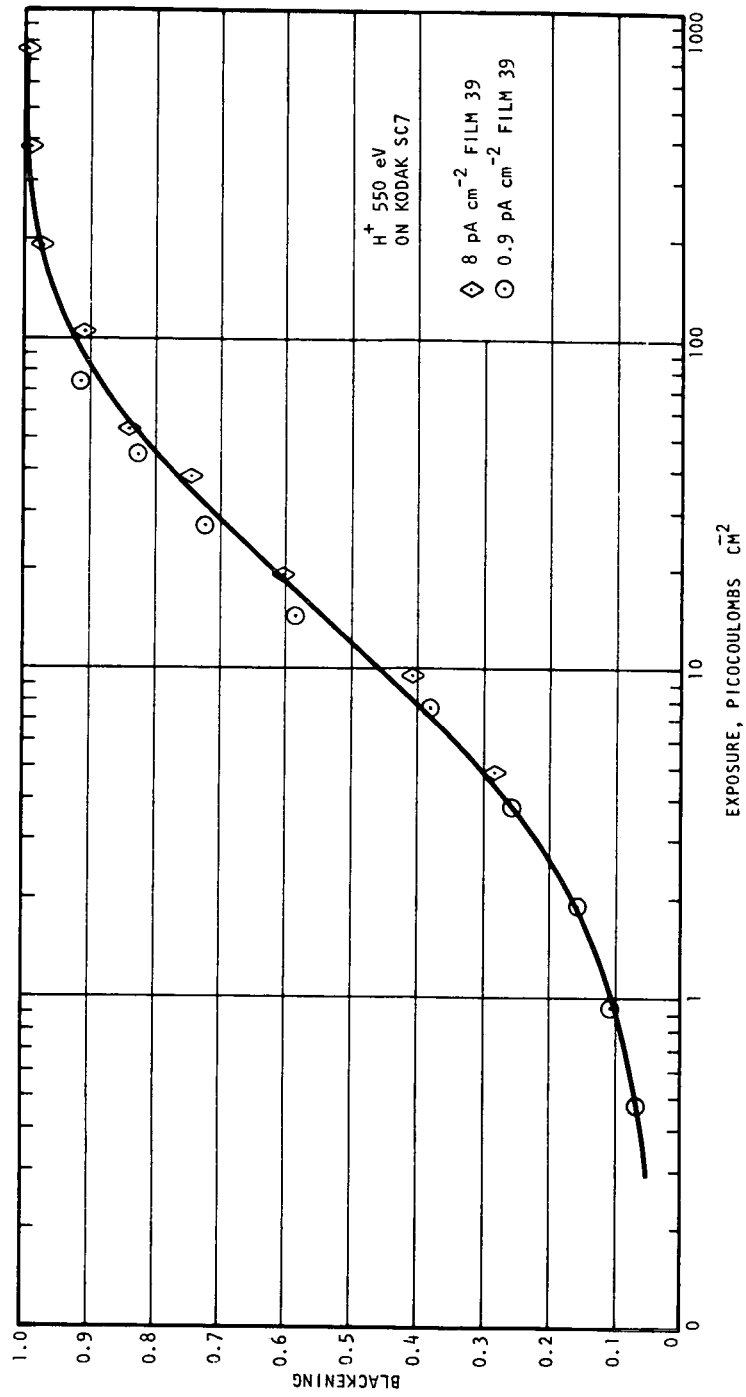


FIGURE 33.- H^+ Kodak (550 eV)

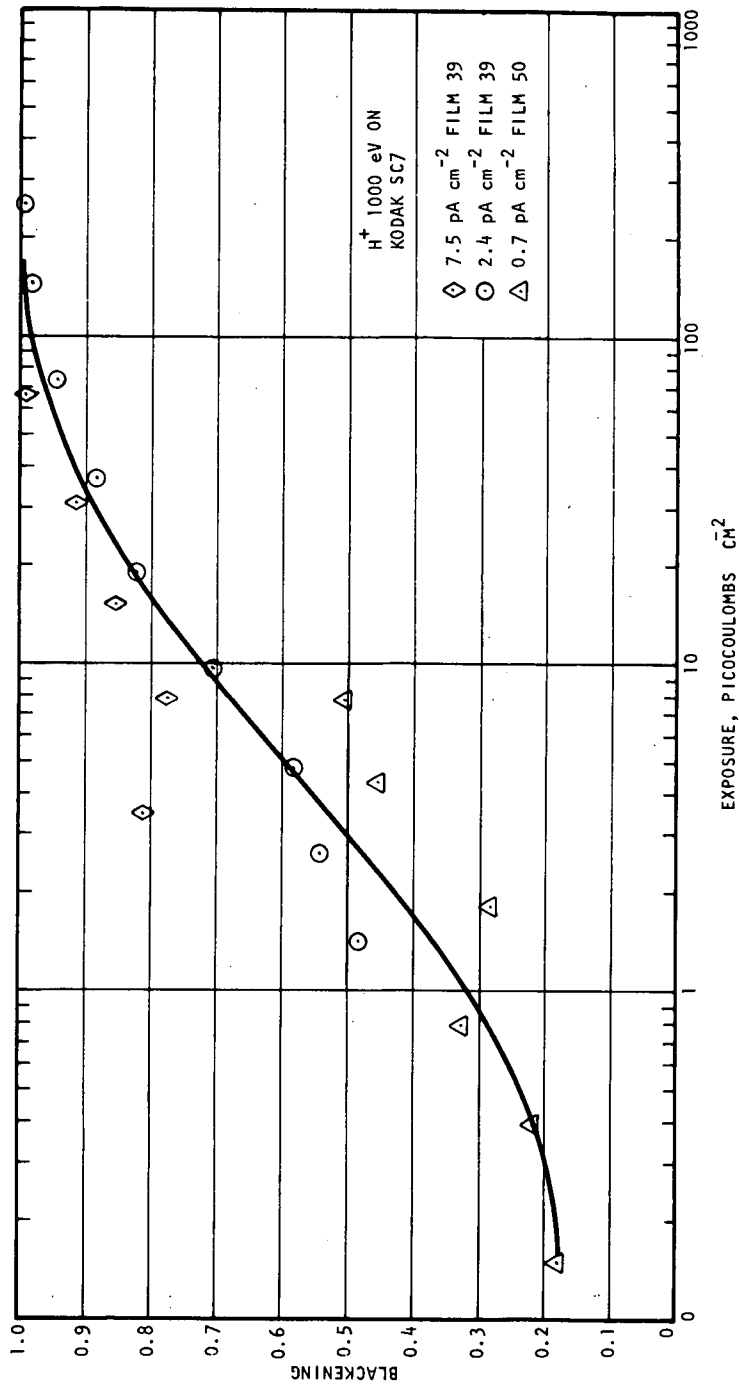


FIGURE 34.- H^+ Kodak (1000 eV)

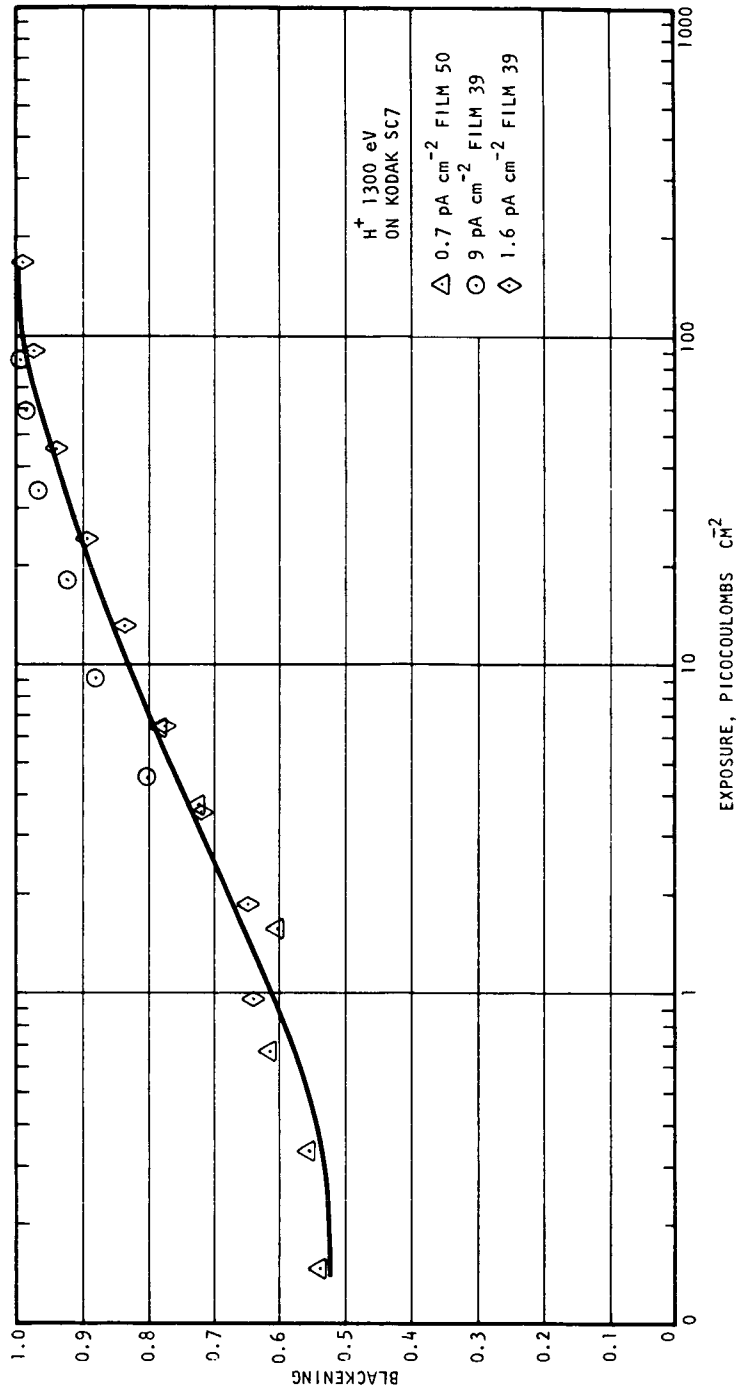


FIGURE 35.- H^+ Kodak (1300 eV)

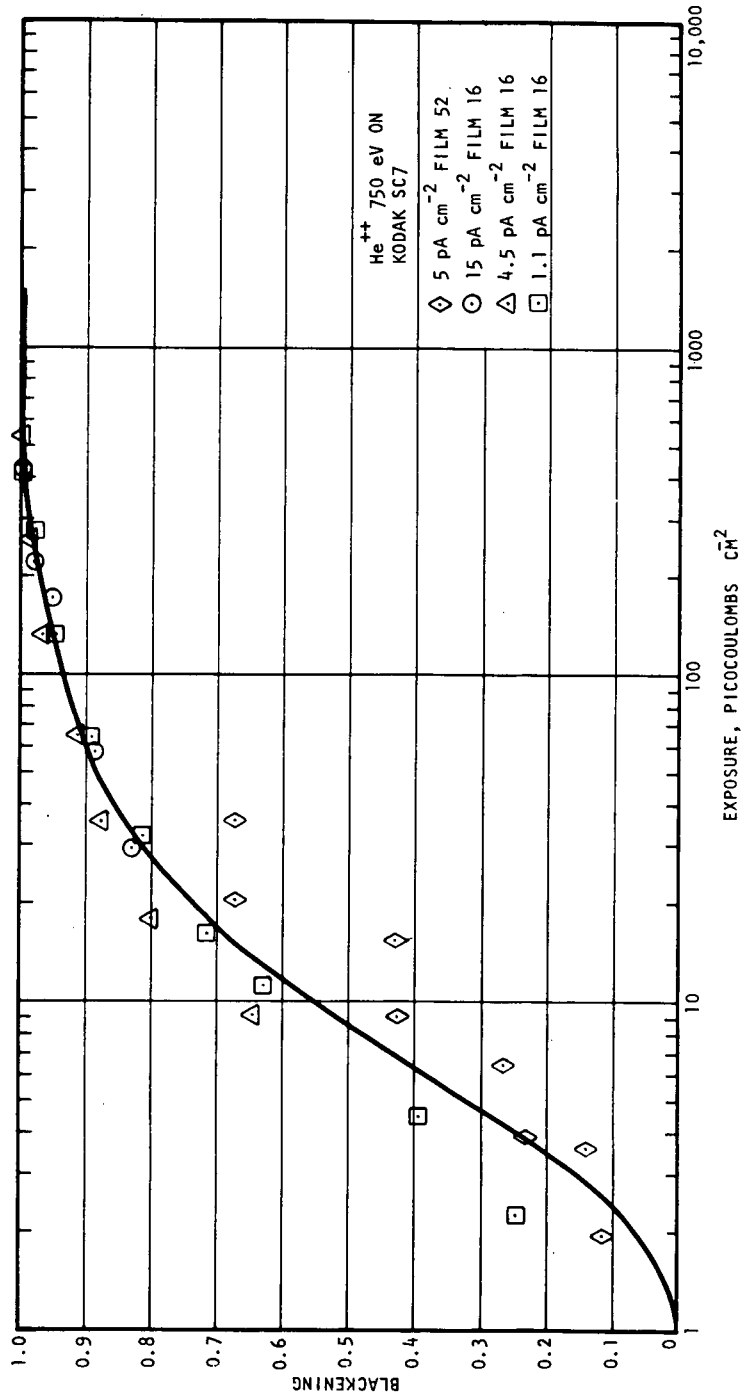


FIGURE 36.- He^{++} Kodak (750 eV)

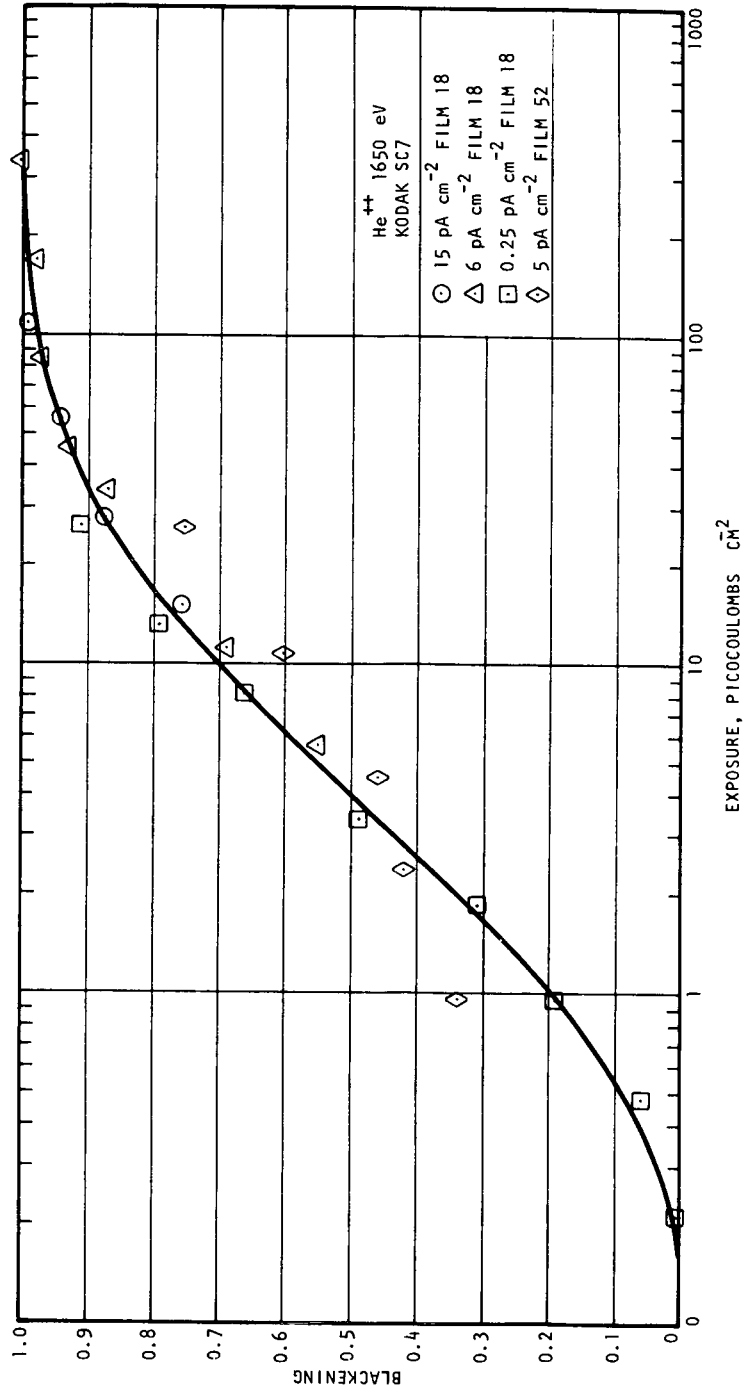


FIGURE 37.- He⁺⁺ Kodak (1650 eV)

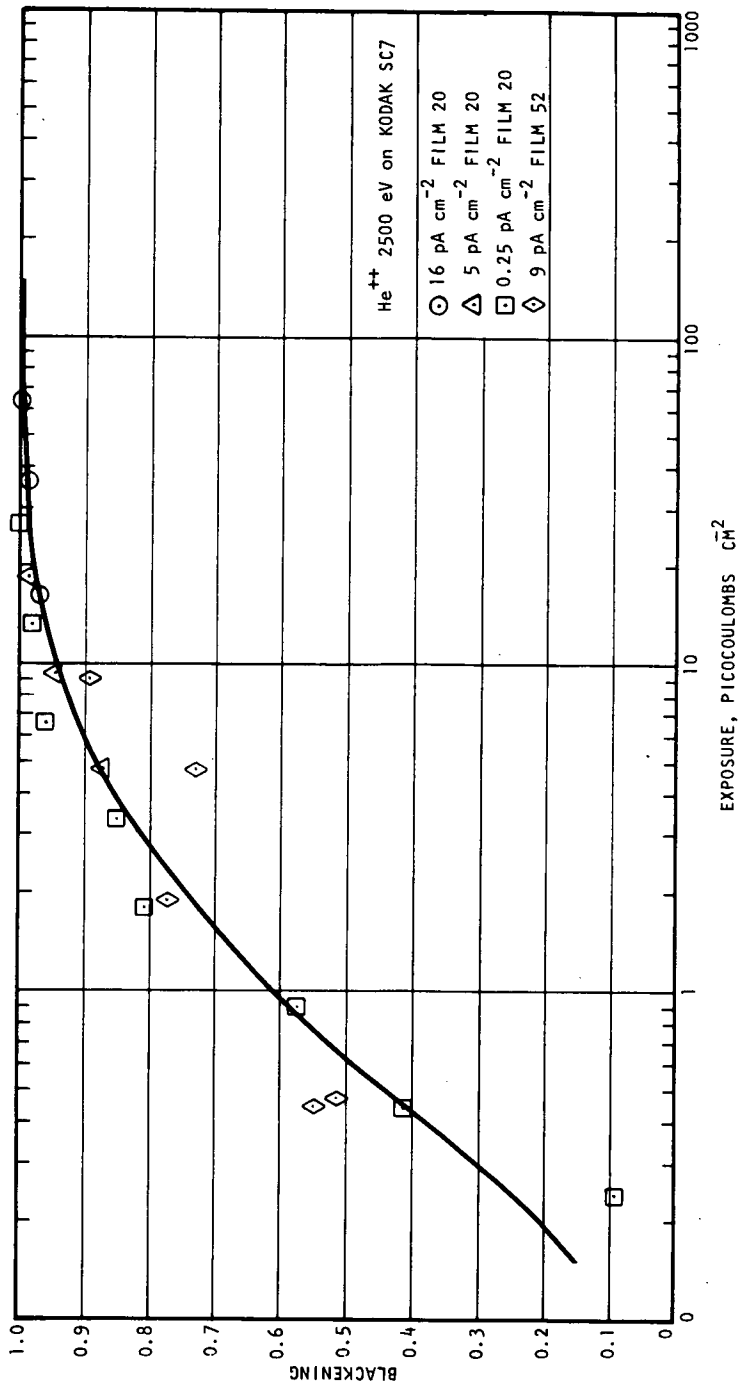


FIGURE 38.- He⁺⁺ Kodak (2500 eV)

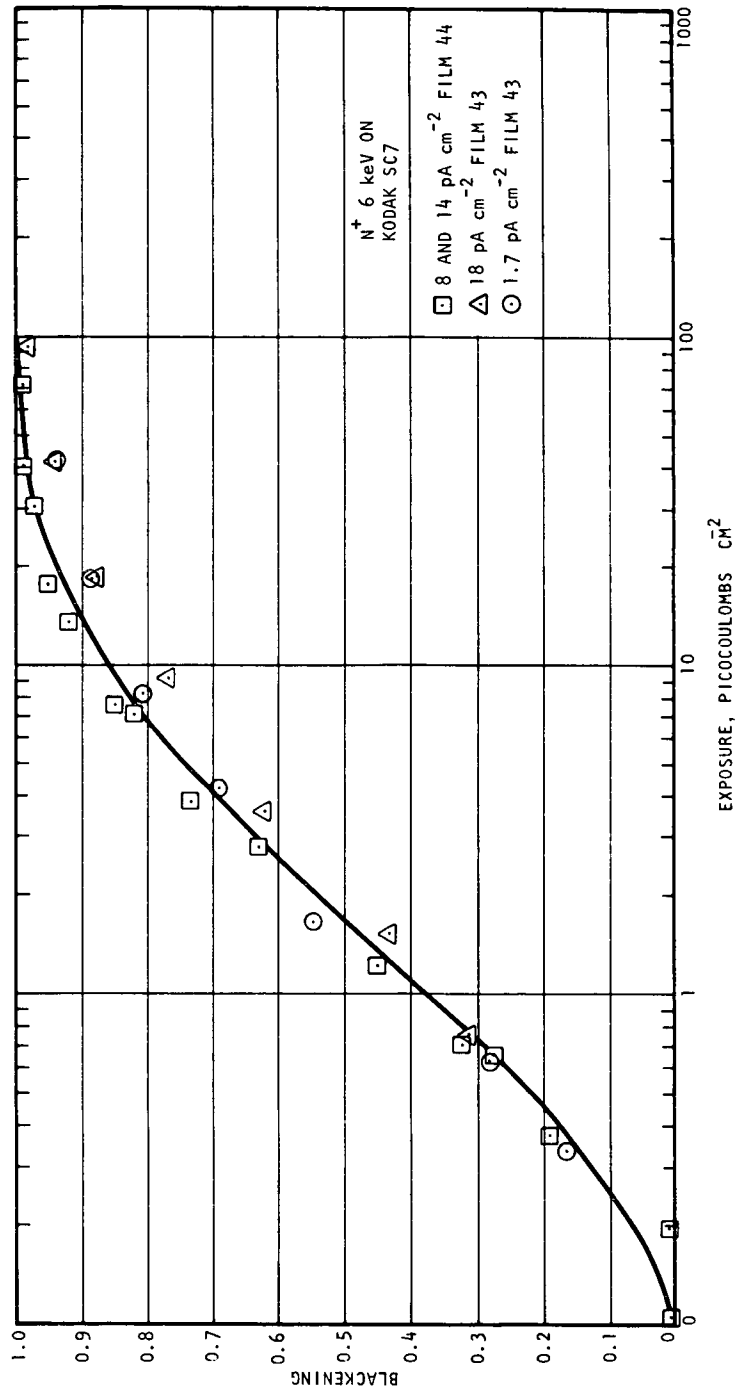


FIGURE 39.- N^+ Kodak (6 keV)

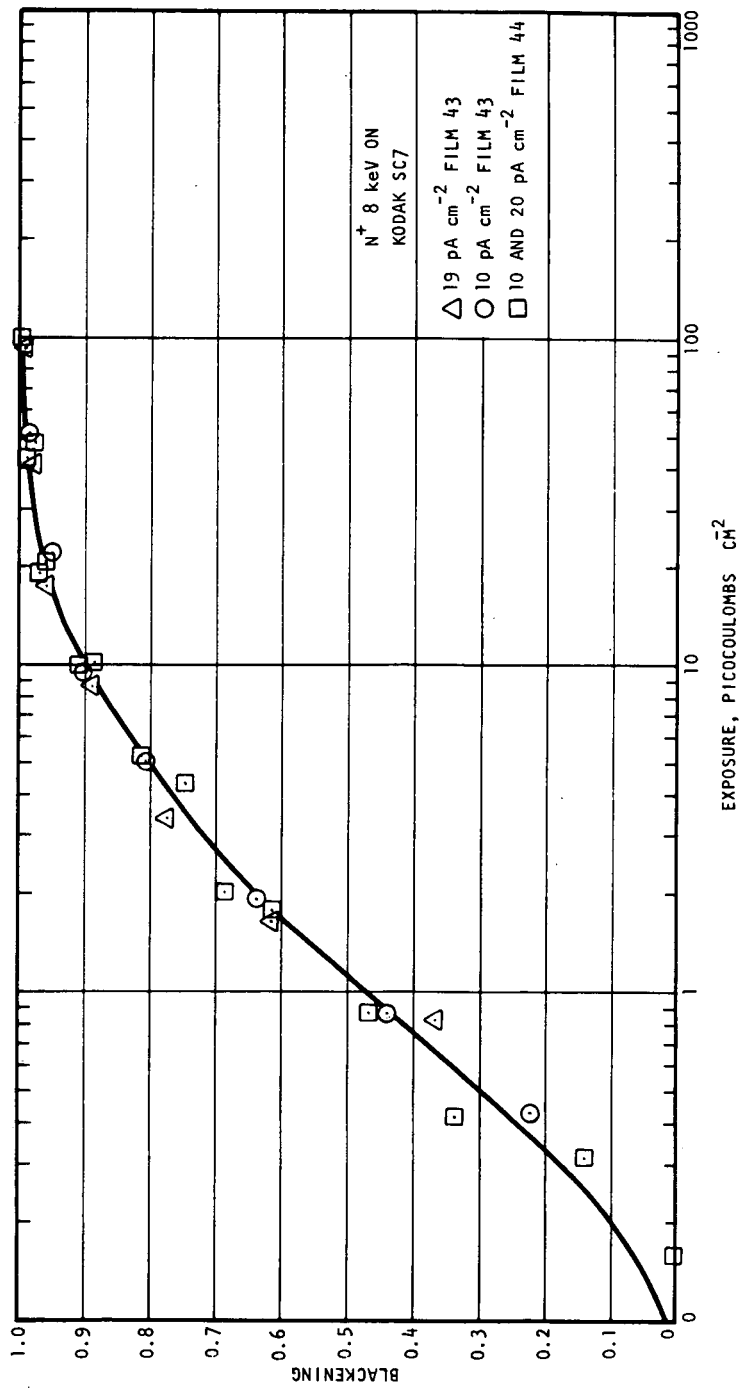


FIGURE 40.- N^+ Kodak (8 keV)

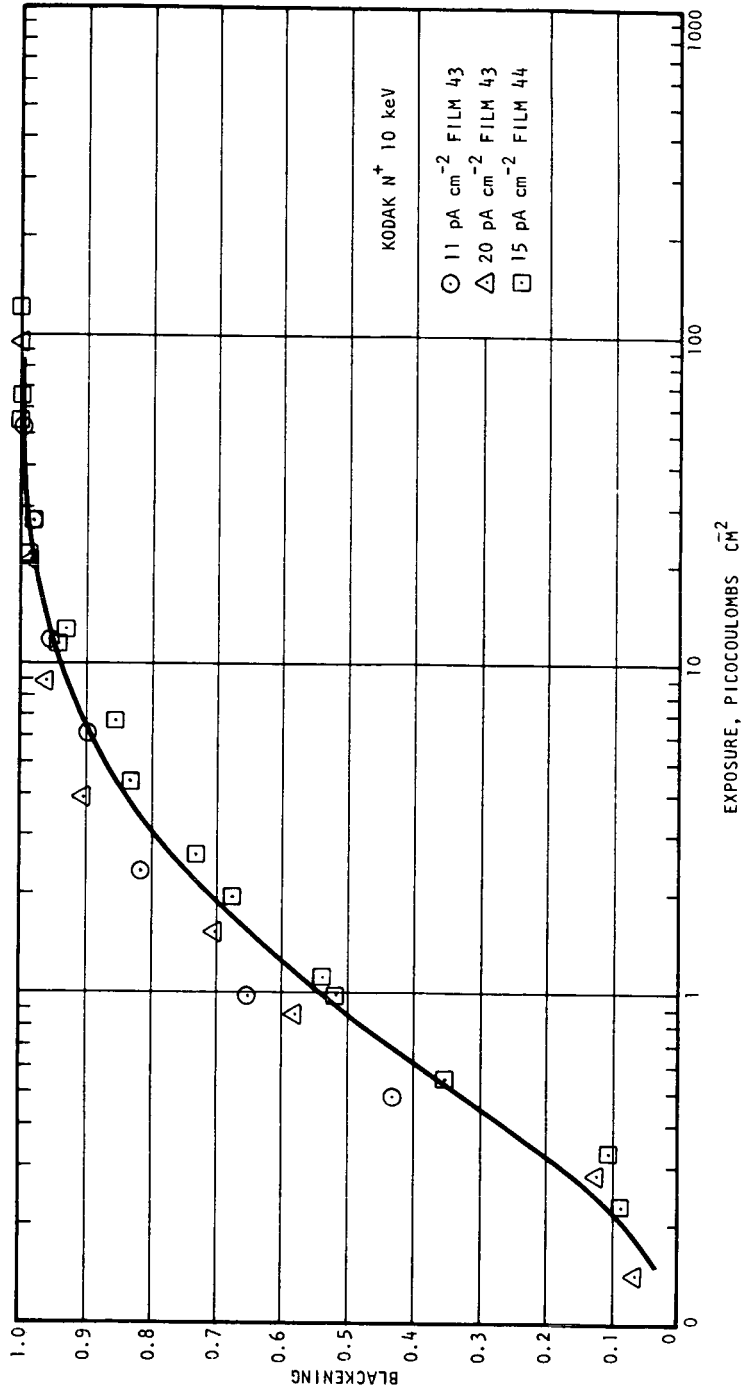


FIGURE 41.- N⁺ Kodak (10 keV)

DO NOT PRINT

APPENDIX B

MEASUREMENT OF CHARACTERISTIC CURVES
FOR KODAK SC7 FILM AND ILFORD Q2 FILM

APPENDIX B

ENGINEERING REPORT NUMBER 6482
MEASUREMENT OF CHARACTERISTIC CURVES
FOR KODAK SC7 FILM AND ILFORD Q2 FILM

11 FEBRUARY 1971

PERKIN-ELMER SALES ORDER NUMBER 30010

APPENDIX B

OBJECT

The object of the test was to measure the characteristic curves for Kodak SC7 film and Ilford Q2 film. The radiant source was to peak at approximately 0.48μ using the closest Wratten filter. The test was to be repeated using various developers and developing times.

DESCRIPTION OF MATERIAL TESTED

The material tested was two types of film used in Solar Ion Mass Spectrometer. The first film tested was a Kodak film (SC7) which is manufactured in France. Kodak's published data is given in Figure 42. The second material tested was a glass film plate manufactured by Ilford (Ilford Q2 film plates) in England. The published data is given in Figure 43.

INSTRUMENTS AND TEST EQUIPMENT

A Gamma Scientific (model 220-9) standard irradiator lamp was used as a source of radiation. The source was calibrated in microwatts/cm² -NM (Figure 44).

A Wratten 48 filter was used to transform the standard irradiator lamp source into a source which peaks at approximately 4800\AA (Figure 45).

An Ilex universal No. 5 shutter was used to control the exposure time. The shutter speed was measured, which resulted in a shutter speed of 0.12 seconds (Figure 46).

A Kodak calibrated step table (No. 906ST417) was used to vary the amount of radiation reaching the film (Figure 47).

APPENDIX B

RESULTS AND CONCLUSION

The digital results of the test are given in the test data section of the report and are also graphed in Figure 48.

The Kodak film developed in D19 developer has a curious hump in the center of the characteristic curve. The hump disappears when developed Microdol X or D-8. The remaining curves have the shape of typical characteristic curve.

DO NOT PRINT

TEST DATA

APPENDIX B

TEST DATA

| Wavelength NM | Spectral Source of Radiation $\frac{\mu \text{ watts}}{\text{cm}^2\text{NM}}$ | Transmission of Wratten 48 Filter | Spectral Source With Wratten 48 Filter $\frac{\mu \text{ watts}}{\text{cm}^2\text{NM}}$ | Spectral Source With Wratten 48 Filter and Shutter (0.12 s) $\frac{\mu \text{ watt s}}{\text{cm}^2\text{NM}}$ | Integration of Spectral Source With Filter and Shutter $\frac{\mu \text{ watt s}}{\text{cm}^2}$ |
|------------------|--|---|---|--|--|
| 395 | 0.06 | 0.0143 | 0.000858 cm^2NM | 0.0001030 | 0.000515 |
| 400 | 0.065 | 0.02 | 0.0013 | 0.000156 | 0.00078 |
| 405 | 0.075 | 0.03002 | 0.00225 | 0.00027 | 0.00135 |
| 410 | 0.085 | 0.045 | 0.00383 | 0.0004596 | 0.00295 |
| 415 | 0.095 | 0.0648 | 0.00616 | 0.000709 | 0.003695 |
| 420 | 0.105 | 0.093 | 0.00977 | 0.001172 | 0.00586 |
| 425 | 0.11 | 0.12 | 0.0132 | 0.00158 | 0.0079 |
| 430 | 0.12 | 0.146 | 0.0175 | 0.00210 | 0.0105 |
| 435 | 0.13 | 0.168 | 0.0218 | 0.00262 | 0.0131 |
| 440 | 0.14 | 0.208 | 0.0291 | 0.00349 | 0.01745 |
| 445 | 0.145 | 0.241 | 0.0350 | 0.0042 | 0.021 |
| 450 | 0.155 | 0.285 | 0.0442 | 0.005304 | 0.02652 |
| 455 | 0.165 | 0.318 | 0.0525 | 0.0063 | 0.0315 |
| 460 | 0.175 | 0.324 | 0.0567 | 0.00681 | 0.0341 |
| 465 | 0.180 | 0.309 | 0.0556 | 0.00667 | 0.03335 |
| 470 | 0.190 | 0.30 | 0.057 | 0.00685 | 0.0342 |
| 475 | 0.20 | 0.262 | 0.0524 | 0.00639 | 0.03145 |
| 480 | 0.21 | 0.221 | 0.0464 | 0.00557 | 0.02785 |
| 485 | 0.22 | 0.1775 | 0.0391 | 0.00469 | 0.02345 |
| 490 | 0.225 | 0.136 | 0.0306 | 0.00367 | 0.01835 |
| 495 | 0.235 | 0.1005 | 0.0236 | 0.00283 | 0.01415 |
| 500 | 0.245 | 0.068 | 0.91666 | 0.001999 | 0.01000 |
| 505 | 0.255 | 0.04 | 0.0102 | 0.00122 | 0.0061 |
| 510 | 0.27 | 0.0182 | 0.0049 | 0.000588 | 0.00294 |
| 515 | 0.28 | 0.0087 | 0.00244 | 0.000293 | 0.00147/0.3799 $\frac{\mu \text{ watts}}{\text{cm}^2}$ |

APPENDIX B

TEST DATA

| Step Tablet | Step Tablet Density | Step Tablet Transmission % | Irradiance To Film $\frac{\mu \text{ watt s}}{\text{cm}^2}$ | Log (Irradiance) To (Film) Log ($\frac{\mu \text{ watt s}}{\text{cm}^2}$) |
|----------------|---------------------------|-------------------------------------|---|---|
| 1 | 0.04 | 91.16 | 0.3463 | -1.53945 |
| 2 | 0.19 | 64.56 | 0.2453 | -1.38970 |
| 3 | 0.34 | 45.70 | 0.1736 | -1.23955 |
| 4 | 0.49 | 32.35 | 0.1229 | -1.08955 |
| 5 | 0.64 | 22.90 | 0.0870 | -2.93952 |
| 6 | 0.78 | 16.60 | 0.0631 | -2.80003 |
| 7 | 0.93 | 11.75 | 0.0446 | -2.64933 |
| 8 | 1.09 | 8.123 | 0.0309 | -2.48996 |
| 9 | 1.25 | 5.62 | 0.0214 | -2.33041 |
| 10 | 1.40 | 3.98 | 0.0151 | -2.17898 |
| 11 | 1.56 | 2.75 | 0.0105 | -2.02119 |
| 12 | 1.72 | 1.91 | 0.00726 | -3.86094 |
| 13 | 1.88 | 1.318 | 0.0050 | -3.69897 |
| 14 | 2.04 | 0.912 | 0.00347 | -3.54033 |
| 15 | 2.2 | 0.631 | 0.00240 | -3.38021 |
| 16 | 2.36 | 0.436 | 0.00166 | -3.22011 |
| 17 | 2.52 | 0.302 | 0.00115 | -3.06070 |
| 18 | 2.68 | 0.209 | 0.00079 | -4.89763 |
| 19 | 2.83 | 0.148 | 0.00056 | -4.74819 |
| 20 | 2.98 | 0.105 | 0.00040 | -4.60206 |
| 21 | 3.13 | 6.0741 | 0.000282 | -4.45025 |

APPENDIX B

TEST DATA

| Step Tablet | D-19 3 Min | D-19 6 Min | D-19 9 Min | D-19 12 Min | Microl-X 30 Min | D-8 2 Min | D-19 3 Min | D-19 6 Min | D-8 2 Min |
|----------------|---------------|---------------|---------------|----------------|--------------------|--------------|---------------|---------------|--------------|
| 1 | 1.48 | 1.44 | 1.44 | 1.56 | 1.03 | 1.66 | 1.72 | 1.49 | 1.90 |
| 2 | 1.46 | 1.42 | 1.39 | 1.50 | 1.01 | 1.54 | 1.70 | 1.49 | 1.88 |
| 3 | 1.40 | 1.41 | 1.35 | 1.45 | 0.98 | 1.45 | 1.64 | 1.47 | 1.83 |
| 4 | 1.31 | 1.42 | 1.32 | 1.38 | 0.95 | 1.38 | 1.58 | 1.45 | 1.75 |
| 5 | 1.20 | 1.38 | 1.26 | 1.26 | 0.98 | 1.27 | 1.49 | 1.38 | 1.66 |
| 6 | 1.09 | 1.34 | 1.21 | 1.21 | 0.85 | 1.22 | 1.37 | 1.34 | 1.55 |
| 7 | 1.03 | 1.27 | 1.16 | 1.21 | 0.81 | 1.19 | 1.28 | 1.25 | 1.40 |
| 8 | 0.93 | 1.16 | 1.13 | 1.06 | 0.78 | 1.12 | 1.19 | 1.13 | 1.24 |
| 9 | 0.90 | 1.10 | 1.06 | 1.08 | 0.74 | 1.07 | 1.03 | 1.00 | 1.07 |
| 10 | 0.89 | 1.01 | 1.03 | 1.14 | 0.70 | 1.01 | 0.90 | 0.86 | 0.90 |
| 11 | 0.78 | 0.99 | 1.03 | 1.19 | 0.66 | 0.92 | 0.66 | 0.72 | 0.71 |
| 12 | 0.72 | 0.92 | 1.01 | 1.12 | 0.60 | 0.76 | 0.43 | 0.60 | 0.52 |
| 13 | 0.68 | 0.85 | 1.03 | 1.08 | 0.52 | 0.64 | 0.28 | 0.42 | 0.37 |
| 14 | 0.59 | 0.72 | 0.95 | 1.04 | 0.46 | 0.48 | 0.20 | 0.30 | 0.28 |
| 15 | 0.49 | 0.66 | 0.79 | 0.91 | 0.42 | 0.35 | 0.15 | 0.23 | 0.22 |
| 16 | 0.40 | 0.59 | 0.65 | 0.71 | 0.34 | 0.24 | 0.12 | 0.17 | 0.18 |
| 17 | 0.28 | 0.49 | 0.47 | 0.52 | 0.28 | 0.17 | 0.10 | 0.15 | 0.16 |
| 18 | 0.19 | 0.33 | 0.36 | 0.38 | 0.22 | 0.13 | 0.10 | 0.12 | 0.14 |
| 19 | 0.16 | 0.22 | 0.34 | 0.34 | 0.18 | 0.12 | 0.10 | 0.12 | 0.12 |
| 20 | 0.11 | 0.20 | 0.34 | 0.34 | 0.18 | 0.12 | 0.16 | 0.12 | 0.12 |
| 21 | 0.09 | 0.20 | 0.34 | 0.34 | 0.18 | 0.12 | 0.10 | 0.12 | 0.12 |
| Base Fog | 0.05 | 0.20 | 0.34 | 0.34 | 0.14 | 0.12 | 0.07 | 0.12 | 0.05 |

APPENDIX B

KODAK PHOTOGRAPHIC EMULSIONS PREPARED BY CENTRIFUGALIZATION FOR USE IN THE FAR ULTRAVIOLET AND MASS SPECTROGRAPHY JULY 1967

The absorption of UV radiation by gelatin is such that the sensitivity of standard photographic emulsions tends to decrease below 0.25μ and to be virtually nil around 0.18μ .

The Kodak-Pathe Research Laboratories have produced a number of films whose sensitivity remains constant even in the far ultraviolet and developed a technique for obtaining by centrifugalization sensitized materials with considerably lower gel content on the surface.

The various materials prepared with this procedure are designed for use in three particular fields:

- (1) Spectrography in the far ultraviolet
- (2) Spectrography in space (which is only one special use of spectrography in the far ultraviolet)
- (3) Mass spectrography.

Three types are at present available.

Kodak Film, Type DC-3

This material contains a fine-grain bromo-iodide emulsion with good definition characteristics and excellent covering power. The micro-contrast of the picture is particularly acute.

Kodak Film, Type SC-5

The sensitivity of this material is higher than that of Kodak Film, type DC-3, but its graininess is slightly more marked. An interesting feature of this film is its low gamma variations according to exposure wavelength.

FIGURE 42.- Kodak SC-7 Test Film (Sheet 1 of 4)

APPENDIX B

Kodak Film, Type SC-7

This film has virtually the same characteristics as Kodak Film, type SC-5, but its sensitivity is slightly higher.

Packing

Kodak Films, types DC-3, SC-5 and SC-7, are normally available in 35 mm-wide, 180 mm-long strips, coated on a flexible triacetate 20/100 mm-thick base.

As these films are not very resistant to abrasion, they are packed in individual plastic film holders preventing any contact with the film surface. Films are grouped by series of 12 in a tin.

Handling, Safelight

These centrifugalized materials must be handled and processed in laboratories with lamps equipped with a Kodak Safelight Filter, Wratten No. 6B (15-watt bulb at not less than 3 feet).

Processing

The recommended developer for processing these films is the Kodak D-19b Developer which yields the best possible contrast with no variation in the threshold value. In special cases when a lower gamma is required, the Kodak DK-20 Developer can be used (see sensitometric curves). The very low gel content at the film surface reduces development time considerably, thus making agitation practically unnecessary. Conversely, the temperature of the processing solution should be kept under careful control and adjusted at 20°C.

Development Time (in Kodak D-19b)

- (1) Kodak Film, type DC-3 - 2 minutes at 20°C
- (2) Kodak Film, type SC-5 - 2 minutes at 20°C
- (3) Kodak Film, type SC-7 - 6 minutes at 20°C

FIGURE 42.- Kodak SC-7 Test Film (Sheet 2 of 4)

APPENDIX B

After processing, the film is rinsed for 10 seconds in running water, fixed for 2 minutes in Kodak Fixing Bath F-5 and washed for 2 minutes in running water.

Great bath-to-bath variations in temperature may cause partial emulsion stripping on the film edges. It is therefore recommended to rinse and wash in running water at 20°C.

Film Strip Protection After Processing

After processing, the surface of the film appears matt and easily subject to abrasion marks; the unexposed parts of the film have a milky appearance due to light diffusion at the surface of the gel coat.

It is recommended to soak the film strips in a varnish to be prepared as follows:

Dissolve: 5 g of cellulose acetobutyrate in a cellulose compound
5 g of acetone
15 g of ethanol
20 g of butyl acetate
60 g of toluene

Viscosity is 6 centipoises at 20°C.

NOTE

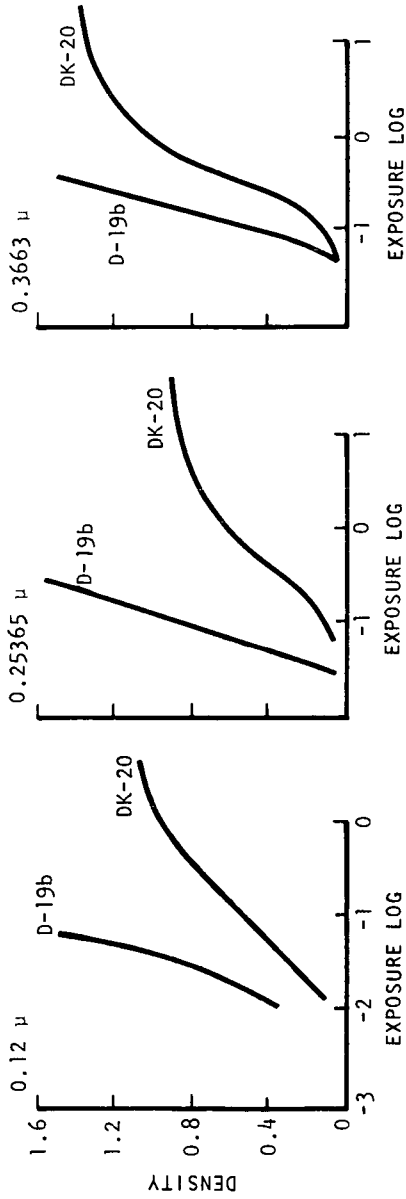
The recommended cellulose acetobutyrate is type EAD-381, half-second, of the Eastman Kodak Company.

Further to this treatment, the film strips which were translucent become transparent, and the contrast of the silver image is thus intensified.

Sensitometric Curves of the Kodak Film, type SC-5, for various exposure wavelengths (excerpt from "Film Calibration" for Rocket UV Spectrographs, by Messrs. Fowler, Rense, Simmons. Applied Optics, Vol. 4, No. 12, Dec 1965).

FIGURE 42.- Kodak SC-7 Test Film (Sheet 3 of 4)

APPENDIX B



Continuous-line curves were plotted for a 2 minute development in D-19b at 20°C. The dotted line curve was plotted for a 12 minute development in DK-20 at 20°C.

Use of Kodak Film, type SC-5, in mass spectrometry. Sensitometric curve plotted with a mass spectrum of a very pure iron sample (after a communication from Messrs. Gavaud, Stéfani, Bourpalliot), (W. Avad. B. Paris, + 26), October 17, 1966.

Sensitivity variation of Kodak Films, type SC-5, according to the exposure wavelengths.

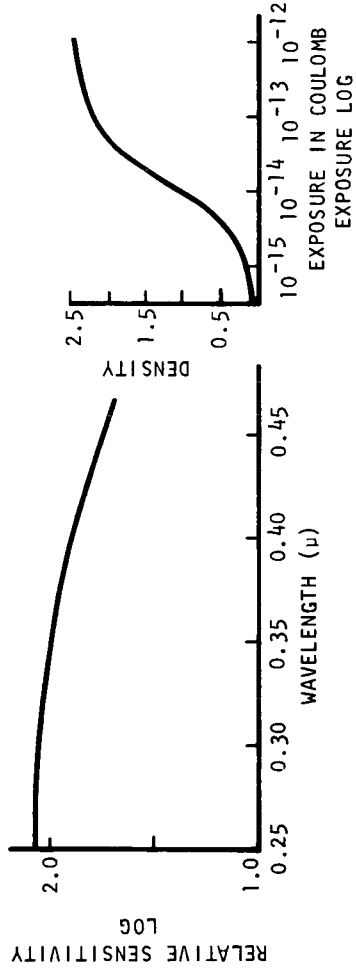


FIGURE 42.- Kodak SC-7 Test Film (Sheet 4 of 4)

APPENDIX B

ILFORD Q PLATES

General Description

Q plates are intended for recording radiation which is absorbed by gelatin such as heavy atomic particles (as in mass spectrography) and ultraviolet radiation of wavelength below 220 Å. For other, more normal radiation they are not recommended because of the fragility of their emulsion surface.

Handling

The emulsion surface of these plates is easily damaged by any rubbing contact. The plates must therefore be handled with great care at all stages, before, during and after processing.

Safelight

Use Ilford F Safelight, No. 904 (dark brown), in an Ilford Darkroom Lamp with the recommended bulb.

Development

For general work use either Ilford Caustic Hydroquinone or ID-19 developer. Both are available as Ilford packed developers. Alternatively, ID-19 may be made up to the published formula. The recommended development time at 20°C (68°F) with continuous agitation is 2-1/2 to 3 minutes for Caustic Hydroquinone and 3-1/2 to 5 minutes for ID-19.

Where maximum contrast is required, Ilford Caustic Hydroquinone should be used. Alternatively, Ilford ID-13 developer may be made up to the published formula. A development time of 2-1/2 to 3 minutes at 20°C (68°F) is recommended.

FIGURE 43.- Ilford Q2 Test Film (Sheet 1 of 2)

APPENDIX B

Fixation and Washing

Ilfofix is recommended. This is available packed in powder form. Alternatively Ilford IF-2 may be made up to the published formula.

Because of the fragile nature of the emulsion, the plates should be fixed for about 5 minutes only, then washed for about 8 minutes only. A final rinse in water to which Ilford Wetting Agent has been added will aid rapid, uniform drying.

FIGURE 43.- Ilford Q2 Test Film (Sheet 2 of 2)

APPENDIX B

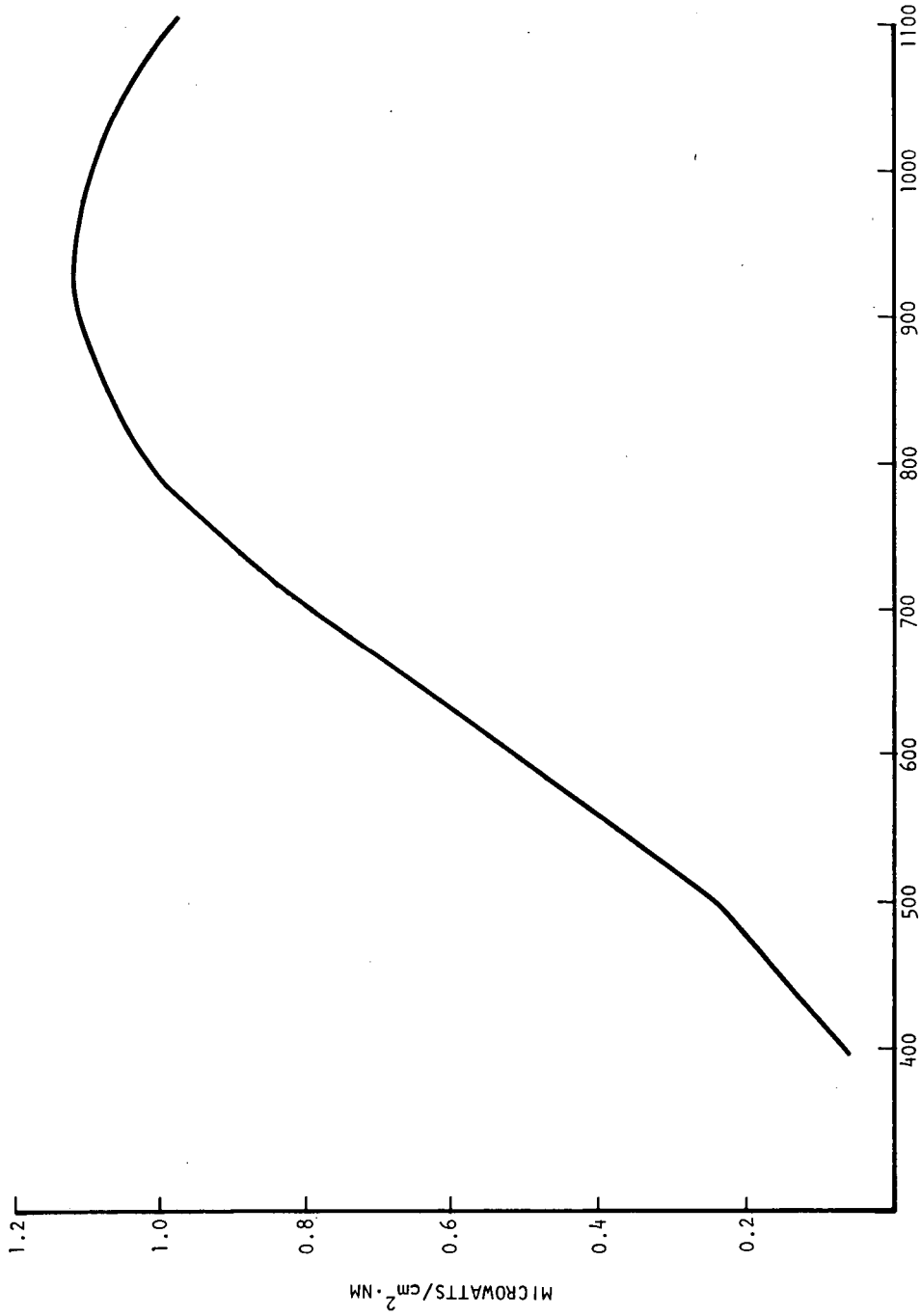


FIGURE 44.- Source Calibration

APPENDIX B

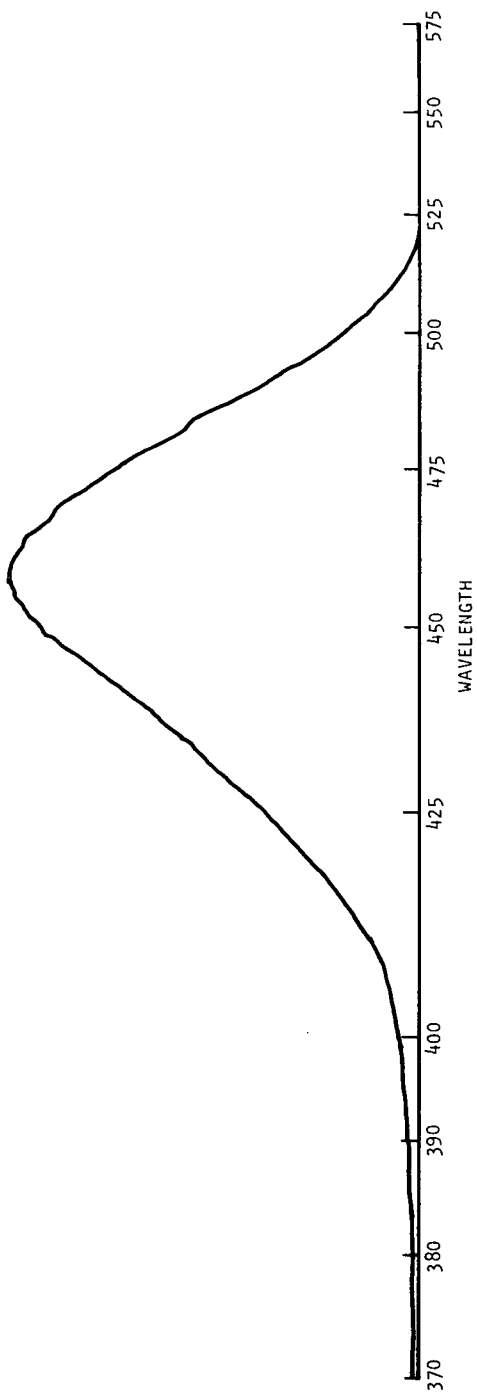


FIGURE 45.- Results Using Wratten 48 Filter

APPENDIX B

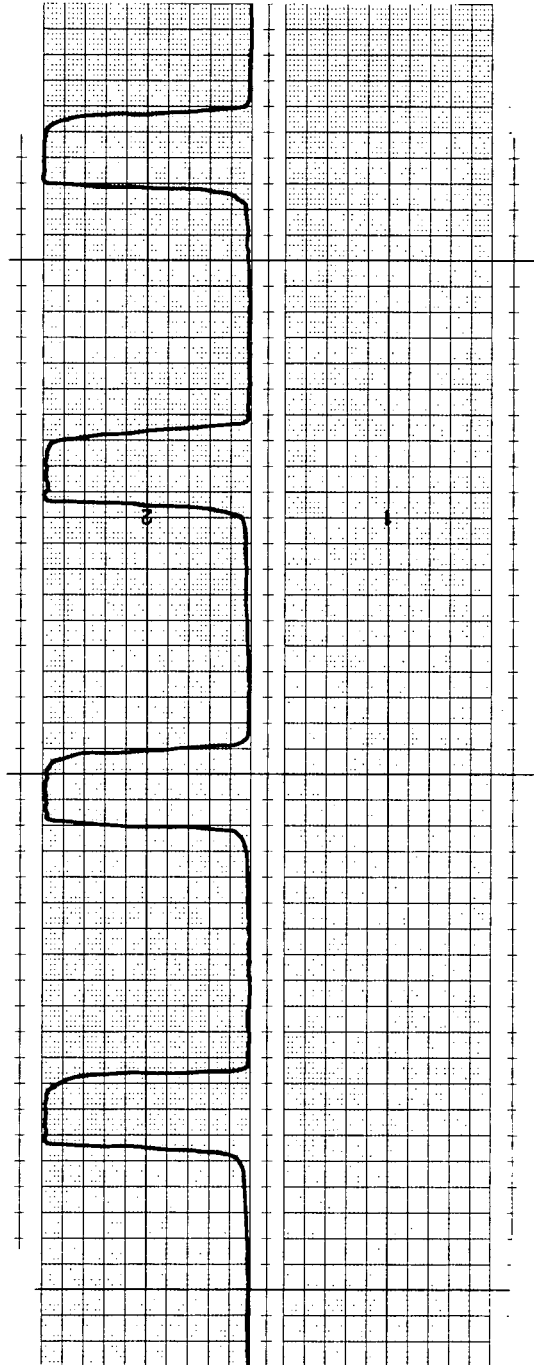


FIGURE 46.- Shutter Speed Measurements

APPENDIX B

| Step | Diffuse Density | Anti Log | $\frac{1}{\text{Anti Log}}$ | Step | Diffuse Density | Anti Log | $\frac{1}{\text{Anti Log}}$ | Step | Diffuse Density | Anti Log | $\frac{1}{\text{Anti Log}}$ |
|------|-----------------|----------|-----------------------------|------|-----------------|----------|-----------------------------|------|-----------------|----------|-----------------------------|
| 1 | 0.04 | 0.1097 | 91.16 | 8 | 1.09 | 1.231 | 8.123 | 15 | 2.20 | 15.85 | 0.631 |
| 2 | 0.19 | 0.1544 | 64.56 | 9 | 1.25 | 1.779 | 5.62 | 16 | 2.36 | 22.91 | 0.436 |
| 3 | 0.34 | 0.2188 | 45.70 | 10 | 1.40 | 2.512 | 3.98 | 17 | 2.52 | 23.12 | 0.302 |
| 4 | 0.49 | 0.3091 | 32.35 | 11 | 1.56 | 3.631 | 2.75 | 18 | 2.68 | 47.87 | 0.209 |
| 5 | 0.64 | 0.4366 | 22.90 | 12 | 1.72 | 5.249 | 1.91 | 19 | 2.83 | 67.61 | 0.148 |
| 6 | 0.78 | 0.6026 | 16.60 | 13 | 1.88 | 7.586 | 1.318 | 20 | 2.98 | 95.50 | 0.105 |
| 7 | 0.93 | 0.8512 | 11.75 | 14 | 2.04 | 10.97 | 0.912 | 21 | 3.13 | 134.9 | 0.0741 |

Calibrated by: *K. E. Smith*
 Kodacolor Processing Division

FIGURE 47.- Kodak Calibration Table

APPENDIX B

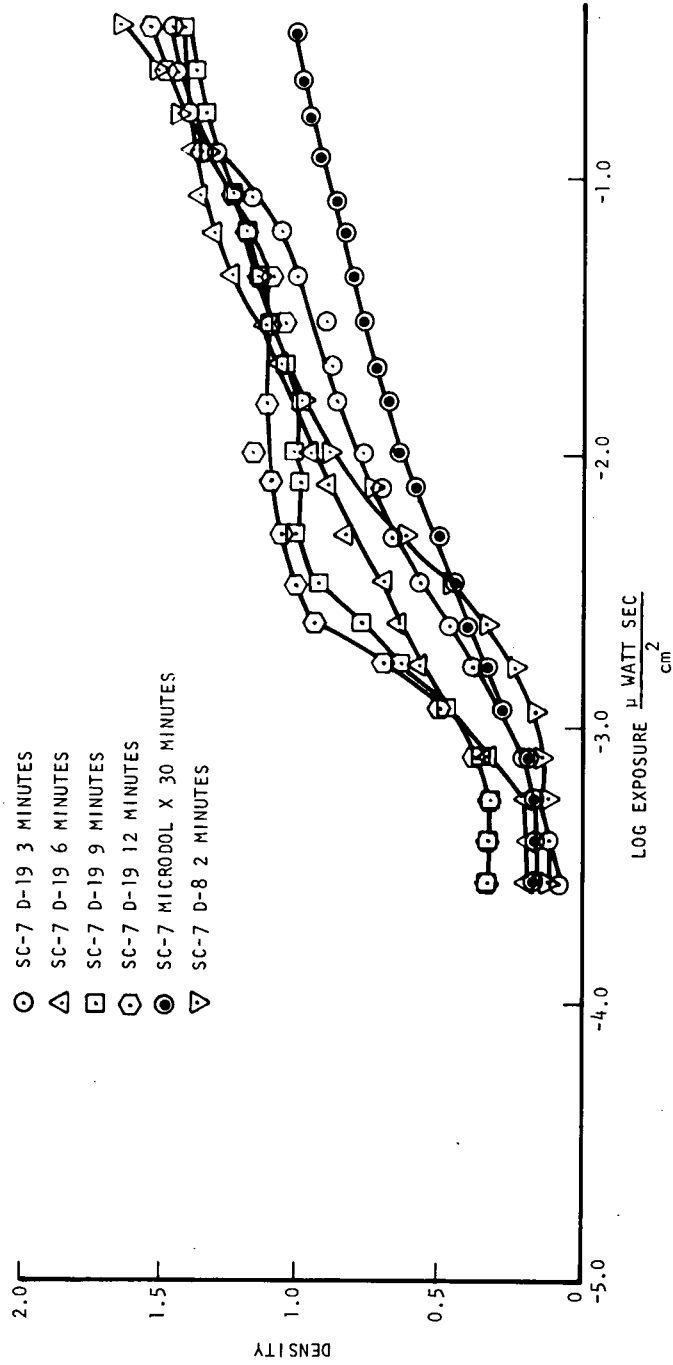


FIGURE 48.- Digital Test Results (Sheet 1 of 2)

APPENDIX B

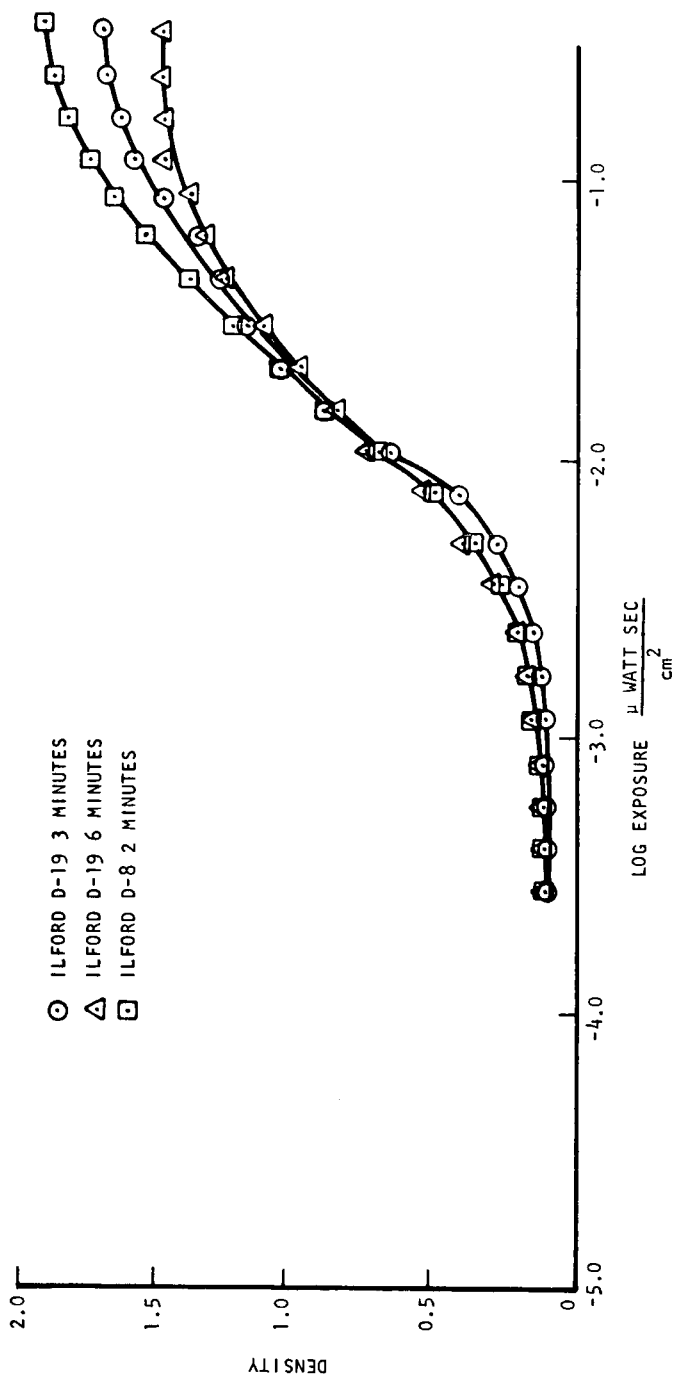


FIGURE 48.- Digital Test Results (Sheet 2 of 2)

REFERENCES

- 1 J.M. McCrea, Ion Sensitive Plate Detectors in Mass Spectrometry, Proceedings Eighteenth Conference ASMS, p B326, (1970)
- 2 W. Finkelberg and W. Humbach, *Naturwissenschaften*, 42, 35 (1955)
- 3 Khairi I, Grais, Mass Dependence of the Factor (R) in Hull's Equation Part II, *Japan Journal of Applied Physics*, 8, 953, (1969)
- 4 Earl W. McDaniel, Collision Phenomena in Ionized Gases, p 190 John Wiley and Sons, N.Y. (1964)
- 5 H.W. Werner and J.M. Nieuwenhuizen, On The Distribution of AgBr Grains in Photographic Plates for Ion Detection in Mass Spectrometers, *2. Naturforchg* 22a, 1035 (1967)
- 6 W.Z. Rudolff
2. Naturforchg 17, 414, (1962)
- 7 J.M. McCrea, Characteristics of Ion Sensitive Emulsions for Mass Spectrometry II, *Applied Spectroscopy* 21, 305, (1967)
- 8 J.R. Woolsten, R.E. Honig, and E.M. Botnick, Response of Ion Sensitive Plates as a Function of Ion Energy, *Rev. Sci. Inst.* 39, 1708, (1967)
- 9 J. Ehrlich, Ilford Research Laboratories, private communication
- 10 A. Cavard, Improvements in Ion Detection by Photographic Development Processes, *Advances in Mass Spectrometers* 4, 419 (1968)
- 11 L.E. Kenneth Mees, Ed., *The Theory of the Photographic Process*, MacMillan Co., N.Y. p 194 (1966)
- 12 L.E. Kenneth Mees, Ed., *The Theory of the Photographic Process*, MacMillan Co., N.Y. p 342 (1966)
- 13 Kodak Plates and Films for Science, Eastman Kodak Company (1967) and Processing Chemicals and Formulas, Eastman Kodak Company (1963)
- 14 J.B. Clegy, Reduction in Secondary Ion Fogging on Photographic Plates Used in Mass Spectrography, *Analytical Chemistry*, 44, 1100, (1972)